

# And the Rest: The Stellar Archeological Record of M82 Outside the Central Starburst<sup>1</sup>

T. J. Davidge

*Herzberg Institute of Astrophysics,  
National Research Council of Canada, 5071 West Saanich Road,  
Victoria, BC Canada V9E 2E7  
email: tim.davidge@nrc.ca*

## ABSTRACT

Deep images obtained with MegaCam and WIRCam on the Canada-France-Hawaii Telescope (CFHT) are used to probe the stellar content outside of the central star-forming regions of M82. Stars evolving on the asymptotic giant branch (AGB) are traced along the major axis out to projected distances of 12 kpc, which corresponds to 13 disk scale lengths. The numbers of red supergiants (RSGs) and AGB stars normalized to local surface brightness (the ‘specific frequency’ – SF) is constant when  $R_{GC} > 4$  kpc, indicating that RSGs and AGB stars are well mixed throughout the disk. Moreover, the SF of bright AGB stars in the outer disks of M82 and the Sc galaxy NGC 2403 are identical, suggesting that the specific star formation rates (SFR) in these galaxies during intermediate epochs were similar. This similarity in stellar content, coupled with the presence of an extended stellar disk, is consistent with M82 having been a late-type disk galaxy prior to interacting with M81. Still, there is a paucity of RSGs in the outer disk of M82 when compared with NGC 2403, indicating that the SFR in the outer regions of M82 during the past  $\sim 0.1$  Gyr has declined dramatically with respect to that in isolated late-type galaxies. The stellar content off of the M82 disk plane is also investigated. A mixture of bright main sequence stars, RSGs, and AGB stars are detected out to minor axis distances of 7 kpc. These stars, which span a range of ages, are concentrated along the outflow. The brightest extraplanar AGB stars define a system with an exponential scale height of  $1.8 \pm 0.2$  kpc, as measured along the minor axis. It is suggested that the young

---

<sup>1</sup>Based on observations obtained with the Mehaprime/MegaCam, a joint project of the CFHT and CEA/DAPNIA, at the Canada-France-Hawaii Telescope, which is operated by the National Research Council of Canada, the Institut National des Sciences de l’Univers of the Centre National de la Recherche Scientifique of France, and the University of Hawaii.

and intermediate aged stars in the extraplanar regions formed in structures similar to M82 South, and that these were subsequently disrupted by the tidal action of M82.

*Subject headings:* galaxies: individual M82 – galaxies: evolution – galaxies: starburst

## 1. INTRODUCTION

The properties of most nearby large galaxies were almost certainly defined by mergers and interactions that occurred during early epochs. Depending on factors such as the gas fraction of the progenitors, their mass ratios, and their relative orbital characteristics, mergers and tidal interactions can dramatically alter the morphologies of the initial systems (e.g. Barnes 1992; Mayer et al. 2001; Springel & Hernquist 2005). Even in cases where the basic structural properties of the progenitors are not altered, galaxy-galaxy interactions can trigger enhanced levels of star formation (e.g. Larson & Tinsley 1978, Iono, Yun, & Mihos 2004, Kewley, Geller, & Barton 2006), thereby altering the appearance of galaxies.

Simulations predict that the bulk of the merger activity associated with the assembly of the Galaxy concluded  $\sim 9$  Gyr in the past (Bullock & Johnston 2005), and signatures of this eventful period may still be seen in the Galactic disk (e.g. Kazantzidis et al. 2007). Still, mergers and interactions continue to occur in the local universe, albeit at a more subdued level than during earlier epochs. As the nearest ensemble of galaxies in which there is evidence of on-going galaxy-galaxy interactions, the M81 group is an unprecedented laboratory for probing the impact of these encounters. Arguably the most dramatic evidence of interactions between M81 and its companions that has been presented to date comes from studies of neutral hydrogen. The HI around M81 and M82 has a disturbed morphology, and HI filaments link M81 with other members of the group (e.g. Brouillet et al. 1991; Yun, Ho, & Lo 1994; Boyce et al. 2001). The distribution of gas suggests that a dramatic event occurred, and timing arguments, in which the galaxy Ho IX is assumed to be a tidal fragment, suggest that M82 passed through the western disk of M81  $\sim 2 \times 10^8$  years in the past (Yun et al. 1994).

The stellar content of M82 constitutes a fossil record that can be mined to probe the nature of the galaxy before it interacted with M81. Studies of the stellar content can also be used to measure the timing of the interactions with M81 by searching for past changes in the SFR. The vast majority of previous studies have focused on the central few kpc of M82, which is a region of intense star-forming activity. Dust largely obscures this part of

M82, and so much work has focused on studies of star clusters in areas that have relatively low extinction (O’Connell et al. 1995), or of the integrated light. The star formation history deduced from star clusters (e.g. de Grijs, O’Connell, & Gallagher 2001) and the visible integrated light spectrum (Mayya et al. 2006) suggest that elevated levels of star formation in M82 commenced some 0.5 – 1.0 Gyr ago. These studies also suggest that the spatial location of star-forming activity has changed with time, in the sense that the area of active star formation has contracted since the initial interaction with M81. Star formation at radii larger than  $\sim 1$  kpc in the M82 disk may have stopped some 0.5 Gyr in the past (Mayya et al. 2006), while the most recent star-forming activity in the inner regions of the disk occurred only a few Myr ago (Gallagher & Smith 1999; Forster Schreiber et al. 2003; Smith et al. 2006).

Given the compelling nature of the central star-forming regions it is perhaps not surprising that there have only been a few studies of the rest of M82. In what has been the largest areal study to date of resolved stars in M82, Sakai & Madore (1999) used images recorded with WFPC2 to study red giant branch (RGB) stars in two adjoining fields in the eastern half of the galaxy. They find a distance modulus of 27.95 based on the brightness of the RGB-tip. A number of luminous candidate asymptotic giant branch (AGB) stars were also identified, hinting at star-forming activity during intermediate epochs.

Davidge et al. (2004) used  $H$  and  $K'$  images recorded with NIRI + ALTAIR on Gemini North to investigate the stellar content at a projected distance of  $\sim 1$  kpc south of the M82 disk plane. The relative numbers of AGB and RGB stars were found to be consistent with stellar evolution models, while the peak brightness of the AGB is consistent with that of an intermediate age population. These data have an angular resolution of 0.08 arcsec FWHM, and the photometric properties of these highly evolved stars are not affected by crowding. These observations suggest that the region off of the M82 disk plane and in the outer disk was an area of recent star formation during the past  $\sim 1$  Gyr, and contains a diverse stellar population.

The extraplanar environment is another region of interest for stellar content studies. The starburst in M82 has triggered an outflow in which at least  $3 \times 10^8 M_{\odot}$  of gas has been ejected from the galaxy (Walter, Weiss, & Scoville 2002). The material in the outflow may interact with clouds of gas and dust that surround M82, which presumably were ejected by earlier outflow events or were pulled from the galaxy during the interaction with M81. Devine & Bally (1999) discuss the ‘Cap’, which is located 11 kpc to the north of M82. The emission from the Cap is thought to be powered by the collision between the outflow and a gas cloud (Lehnert et al. 1999; Strickland et al. 2004). The Cap contains knots at visible wavelengths that may herald the early stages of star formation.

Davidge (2008) investigated the stellar content of a stream of stars  $\sim 6$  kpc south of M82. This feature, which was named ‘M82 South’ by Sun et al. (2005), covers a  $0.3 \times 3.1$  kpc<sup>2</sup> area and has an integrated brightness  $M_V \sim -9.5$ . Individual stars were resolved, and comparisons with isochrones indicate that star formation in M82 South last occurred  $\sim 50$  Myr ago. This age overlaps with the most recent era of large-scale star formation in tidal features throughout the M81 group (e.g. Makarova et al. 2002; Sakai & Madore 2001). The oblong appearance of M82 South and the spatial flaring of stars at its eastern end suggest that it is dispersing, thereby raising the possibility that the young stars in M82 South may diffuse into the extraplanar regions of the galaxy.

There has not yet been a comprehensive survey of the stellar content of the outer disk and extraplanar regions of M82. Such a survey should encompass an area covering at least a few hundred arcmin<sup>2</sup> since (1) the disks of late-type galaxies typically extend out to distances of at least 10 kpc, which translates to an angular distance of 9 arcmin at the distance of M82, and (2) the interface between the outflow and surrounding clouds occurs  $\sim 10$  arcmin from M82 if the Cap is assumed to be a representative example of this phenomenon. In the current paper, the wide-field capabilities of the CFHT MegaCam and WIRCam imagers are used to conduct an initial reconnaissance of the stellar content in the outer disk and the extraplanar regions of M82.

A combined visible + infrared dataset offers significant benefits for investigating the stellar content of a galaxy like M82. The stellar types that dominate at visible and infrared wavelengths are very different. Not only does this enable a more comprehensive census of the most evolved stars, but it also provides a means of assessing the impact of crowding, as the contrast between the brightest objects and the underlying populations differ with wavelength. The impact of dust can also be investigated by comparing the photometric properties of stars that are sampled over a wide wavelength range.

A goal of this paper is to investigate the spatial extent and stellar content of the outer disk of M82, as this information provides insight into the nature of the galaxy before – and immediately after – its interaction with M81. The present data sample the semi-major axis of M82 out to the limiting distances at which disk stars have been detected in non-interacting late type galaxies. These are regions where the disk surface brightness is too low to be detected in integrated light, but where individual disk stars can still be identified. The spatial extent of the M82 disk is of interest as Sofue et al. (1992) and Sofue (1998) discuss the rotation curve of M82, and suggest that the dark matter halo and outer disk of the galaxy were stripped away. This interpretation is not ironclad, and needs to be tested by directly measuring the size of the stellar disk. Indeed, a caveat when interpreting velocity measurements in M82 is that the dynamics in the central regions of the galaxy are dominated

by a bar (Wills et al. 2000), which accounts for a significant fraction of the total galaxy mass, and so is a dynamically significant component (e.g. Greve et al. 2002). Moreover, the velocity field defined by the [SIII] 9069 Å line challenges the presence of Keplerian rotation outside of the region affected by the bar (McKeith et al. 1993).

As for the recent star-forming history of the outer disk of M82, if large-scale star formation outside of the central  $\sim 1$  kpc of M82 terminated during intermediate epochs, as predicted by Mayya et al. (2006), then the CMDs of the outer disk should contain a prominent AGB and few – if any – supergiants or bright main sequence stars. The fractional contribution made by supergiants and main sequence stars to the total light in the outer disk of M82 should thus be smaller than in galaxies with on-going star formation. Moreover, if the star burst in M82 was originally global in nature, encompassing much of the disk before retreating to smaller radii, then the number density of AGB stars should also be higher at intermediate and large radii than in a normal late-type galaxy. Is the stellar content of the outer disk of M82 consistent with these expectations?

Another goal of this paper is to investigate the nature and distribution of the brightest objects in the extraplanar regions of M82, as these also provides clues into M82’s past and future. If M82 was a late-type galaxy prior to interacting with M81 then it would have had a modest entourage of globular clusters. These clusters are the brightest tracers of the early history of M82, and the discovery of even a modest globular cluster population in the extraplanar regions would suggest that the interaction with M81 did not strip the outermost stellar regions from the galaxy. In addition, if other stellar collections like M82 South have formed in the recent past then a significant stellar component made up of young and/or intermediate age stars may be present off of the disk plane. The spatial distribution of such stars provides clues into their places of origin. Moreover, if the extraplanar regions are populated with stars that span a range of ages and metallicities then an observer a few Gyr in the future will see M82 as a galaxy with a diverse halo population, as is seen in the halos of some nearby late-type galaxies.

The paper is structured as follows. The acquisition and processing procedures are summarized in §2, along with a description of the photometric measurements. The photometric properties and spatial distribution of stars in the outer disk and extraplanar regions of M82 are discussed in §§3 and 4. A summary and discussion of the results follows in §5.

## 2. OBSERVATIONS AND REDUCTIONS

### 2.1. MegaCam

Deep images of a single MegaCam (Boulade et al. 2003) pointing centered midway between M81 and M82 were recorded through  $r'$ ,  $i'$  and  $z'$  filters on the night of October 23 UT 2006. The detector in Megacam is a mosaic of thirty six  $2048 \times 4612$  pixel<sup>2</sup> CCDs, that together cover an area of one degree<sup>2</sup> with  $0.185$  arcsec pixel<sup>-1</sup>. The data were recorded with a square-shaped dither pattern to assist with the identification of bad pixels and the suppression of cosmic rays. Four 300 sec exposures were recorded in  $r'$  and  $i'$ , while four 500 sec exposures were recorded in  $z'$ . Stars have  $0.7 - 0.8$  arcsec FWHM in the final processed images, depending on the filter.

The removal of instrumental and environmental signatures from the raw images was done with the ELIXIR package at the CFHT. This processing included bias subtraction, flat-fielding, and the subtraction of a fringe frame. The ELIXIR-processed images were then aligned, stacked, and trimmed to the area that is common to all exposures.

### 2.2. WIRCam

Images of M82 were recorded through  $J$ ,  $H$  and  $Ks$  filters with WIRCam (Puget et al. 2004) on the night of February 4 UT 2007. The detector in WIRCam is a mosaic of four  $2048 \times 2048$  HgCdTe arrays. Each exposure covers  $21 \times 21$  arcmin<sup>2</sup>, with  $0.3$  arcsec pixel<sup>-1</sup>.

The WIRCam data were recorded with a square-shaped dither pattern. A total of 20 45 sec exposures were recorded in  $J$ , while 120 15 sec exposures were recorded in  $H$ , and 160 15 sec exposures were recorded in  $Ks$ . The  $J$  data were obtained over one dither cycle (i.e. five 45 sec exposures were recorded per dither position), while the  $H$  and  $Ks$  data were obtained over two dither cycles. Stars in the final images have  $0.8$  arcsec FWHM.

The initial processing of the WIRCam data was done with the I<sup>2</sup>WI pipeline at the CFHT, and this consisted of dark subtraction and flat-fielding. To continue the processing, a calibration frame to remove interference fringes and thermal emission artifacts was constructed by median-combining the I<sup>2</sup>WI-processed M82 images with those of an adjacent field that were recorded immediately after M82. The data were DC sky-subtracted before they were combined to account for exposure-to-exposure variations in sky brightness. In addition, a pixel-by-pixel low-pass clipping algorithm was applied to suppress stars and galaxies in both fields. The resulting calibration frames were subtracted from the flat-fielded data. The processed images were then aligned, stacked, and trimmed to the area that is common

to all exposures.

### 2.3. Photometric Measurements

The photometric measurements were made with the point-spread-function (PSF) fitting program ALLSTAR (Stetson & Harris 1988). The PSF and star catalogues used by ALLSTAR were obtained from DAOPHOT (Stetson 1987) routines. The photometric catalogues were culled in two ways to reject objects with poorly determined photometric measurements. First, all objects in which the fit error ( $\epsilon$ ) computed by ALLSTAR exceeded 0.3 mag were rejected. This removed objects near the faint limit of the data, where photometry is problematic. Second, objects that have an  $\epsilon$  that is markedly higher than the majority of objects with the same brightness were also removed. The objects rejected in this step tend to be either (1) non-stellar, (2) multi-pixel cosmetic defects, and/or (3) in the crowded inner regions of M82.

The photometric measurements were calibrated using standard star observations that were obtained within a few days of the science observations. The MegaCam photometry were calibrated using the zeropoints that are placed in the data headers during ELIXIR processing, which are computed from standard star observations that are obtained during each MegaCam observing run. The WIRCam observations were calibrated using zeropoints published on the CFHT website that were computed from standard star observations made during February 2007.

Artificial star experiments were used to estimate sample completeness, the random scatter in the photometry, and the brightness at which blends of fainter stars account for a significant number of objects. The artificial stars were assigned brightnesses and colors that are consistent with the main locus of stars in M82. As with actual sources, an artificial star was considered to be recovered only if it was detected in at least two filters. The artificial star measurements were subjected to the  $\epsilon$ -based rejection criterion discussed previously.

The results of the artificial star experiments depend on the stellar density, in the sense that as stellar density drops then at a given magnitude (1) the completeness fraction increases, (2) the random scatter in the photometry decreases, and (3) the incidence of interloping blends of fainter stars decreases. For sources in the M82 disk plane, the 50% completeness level in the MegaCam measurements occurs near  $i' = 24.0$  in the 4 – 6 kpc distance interval and  $i' = 24.5$  in the 10 – 12 kpc interval. As for the WIRCam measurements, the 50% completeness level occurs near  $K = 19.8$  in the 4 – 6 kpc distance interval, and  $K = 20$  in the 10 – 12 kpc interval. The completeness fraction is less sensitive to changes

in stellar density in the WIRCam data than in the MegaCam data because of the diminished impact of line blanketing at wavelengths longward of  $1\mu\text{m}$ , which results in greater contrast between AGB stars and the main body of red giant branch and bluer stars in the infrared than the visible. The completeness fractions of stars in the extraplanar regions are comparable to those in the 10 – 12 kpc disk interval. The artificial star experiments indicate that blends can constitute a significant fraction of stars at magnitudes where the completeness fraction is below  $\sim 50\%$ .

### 3. THE OUTER REGIONS OF THE M82 STELLAR DISK

Based on its total mass, luminosity, and stellar content, O’Connell & Manganò (1978) argue that M82 was a late-type disk or irregular galaxy prior to interacting with M81. Morphologically, the spiral structure of M82 is consistent with type SBc (Mayya, Carrasco, & Luna 2005), although there may be structural differences with respect to late-type galaxies in the local Universe. Indeed, if gas in the disk of M82 defines a Keplerian rotation curve out to a radius of  $\sim 4$  kpc (e.g. Sofue et al. 1992; Sofue 1998 – but also the discussion in §1) then M82 lacks (1) a massive halo and (2) an extended stellar disk.

While the observational properties of M82 have undoubtedly been affected by interactions with M81, signatures of its nature prior to this encounter may remain. In this section we seek (1) to measure the spatial extent of the M82 stellar disk, and determine if it is comparable to that in other nearby late-type spirals, which have been traced out to many scale lengths (e.g. Davidge 2007; Bland-Hawthorn et al. 2005), and (2) to determine if the spatial density of old and intermediate age stars is comparable with that of other late-type galaxies. Only stars that are within  $\pm 65$  arcsec of the major axis of M82 are considered. While this criterion excludes stars along the minor axis of M82 that belong to the disk, it reduces contamination from extraplanar stars, some of which appear to have young and intermediate ages (§4).

#### 3.1. An Overview of the CMDs

The  $(i', r' - i')$  and  $(z', i' - z')$  CMDs of stars within  $\pm 65$  arcsec of the major axis of M82 are shown in Figure 1. The stars have been grouped according to projected galactocentric distance in the disk plane, assuming a distance modulus of 27.95 (Sakai & Madore 1999) and a disk inclination of 77 degrees (Mayya et al. 2005). A consequence of the large disk inclination is that the various radial intervals sample comparable projected areas on the sky,



and so the number of contaminating foreground stars and background galaxies is roughly the same in each interval.

The plume of objects with  $r' - i'$  between 0 and 1 and  $i' < 22$  in the top row of Figure 1, and with  $i' - z' \sim 0$  and  $z' < 22$  in the bottom row, consists of Galactic disk stars, although some of the blue objects with  $i' \sim z' > 20$  in the 2 – 4 kpc CMDs could be young and intermediate age star clusters in M82. Stars in M82 dominate the lower half of the CMDs in Figure 1. The concentration of objects that peaks near  $i' \sim 22.5 - 23$  and  $z' \sim 22 - 22.5$  in the  $R_{GC} > 4$  kpc CMDs is made up of stars that are evolving on the AGB, and so have ages  $> 100$  Myr. The AGB sequence is more vertical on the  $(z', i' - z')$  CMDs than the  $(i', r' - i')$  CMDs because of the diminished impact of line blanketing at longer wavelengths. The concentration of AGB stars can be seen in the MegaCam CMDs out to at least  $R_{GC} \sim 10$  kpc, hinting that the stellar disk extends to at least this radius. Background galaxies, which span a range of colors and increase in numbers towards fainter magnitudes, are the largest source of contamination at magnitudes and colors of the AGB component, and make the identification of individual AGB stars in the CMDs at larger radii difficult. The issue of the radial extent of the M82 disk is examined in greater detail in §3.4, where it is demonstrated that a statistically significant excess number of disk AGB stars can be traced out to  $R_{GC} = 12$  kpc.

The  $(K, H - K)$  and  $(K, J - K)$  CMDs of stars along the major axis of M82 are shown in Figure 2. As with the CMDs at shorter wavelengths, foreground Galactic disk stars form a plume of relatively blue objects in the top half of the CMDs. Stars in M82 occur in large numbers when  $K \geq 19$  and – as with the CMDs in Figure 1 – the majority of these are evolving on the AGB. The peak brightness of the AGB in these CMDs ( $K \sim 18.5 - 19$ ) is well above the magnitude where contamination from blends of fainter stars is expected to be an issue (§2.3). As in Figure 1, a concentration of AGB stars can be seen in the near-infrared CMDs out to at least  $R_{GC} = 10$  kpc.

The ridgeline of the bright AGB sequence in M82 has  $H - K \sim 0.4$  and  $J - K \sim 1.3$ . Normal background galaxies at cosmologically modest redshifts tend to have redder colors than these because the first overtone CO bands, which are among the strongest features in the spectrum of highly evolved stars and have a large influence on  $J - K$  and  $H - K$  colors, are shifted out of the  $K$  bandpass when  $z \geq 0.1$ . The mean redshift of galaxies at  $K \sim 17$  is  $\langle z \rangle \sim 0.4$  (Cowie et al. 1996), and a normal galaxy at this redshift will have  $H - K \sim 0.8$  and  $J - K \sim 1.6$  after applying the k-corrections from Mannucci et al. (2001). In fact, collections of objects with such colors are seen in the CMDs of the two outermost intervals in Figure 2. There are objects with  $H - K > 0.5$  and  $J - K > 1.5$  in the CMDs that sample smaller galactocentric distances in Figure 2, and some of these may be C stars in M82 (e.g.

Davidge 2005). However, the reader is cautioned that some of these objects are probably background galaxies rather than stars in M82.

### 3.2. Comparisons with Isochrones

Isochrones with ages  $\log(t_{yr}) = 7.5, 8.0, 8.5,$  and  $9.0$  from Girardi et al. (2002; 2004) are compared with selected  $(i', r' - i')$  and  $(K, J - K)$  CMDs in Figures 3 ( $Z=0.008$ ) and 4 ( $Z=0.019$ ). A distance modulus of 27.95 (Sakai & Madore 1999) is assumed, with  $A_B = 0.12$  mag (Burstein & Heiles 1982). No correction for internal reddening has been applied.

The reddening maps of Schlegel, Finkbeiner, & Davis (1998) indicate that  $A_B = 0.69$  mag for M82, which is considerably higher than the foreground extinction measured by Burstein & Heiles (1982). This difference is undoubtedly due to emission from dust in M82. The dust in M82 is centrally concentrated, and is not expected to be a major influence at large radii. Still, the comparisons in Figures 3 and 4 are not greatly affected by internal extinction as long as the true distance modulus also accounts for any additional source of reddening. For example, if  $A_B = 0.69$  is used to compute a revised ‘true’ distance modulus from the Sakai & Madore (1999) RGB-tip measurement, which is based on observations of stars in the outer disk, then the ages inferred from comparisons with the isochrones differ by only  $\sim 0.1$  dex from those measured if  $A_B = 0.12$  mag is assumed.

The ages inferred for the main locus of AGB stars from the  $Z = 0.008$  and  $Z = 0.019$  sequences differ by 0.5 dex. While the interstellar medium (ISM) and young stars in M82 have metallicities approaching (e.g. Martin 1997; Gallagher & Smith 1999) and even exceeding (Origlia et al. 2004) solar, the metallicities of stars that formed during intermediate epochs are almost certainly lower than those of younger stars. Parmentier et al. (2003) estimated metallicities for clusters in M82, and these data indicate that clusters with ages  $\log(t) = 8.0$  have slightly sub-solar metallicities, while clusters with  $\log(t) = 8.5$  have  $Z = 0.008$  (e.g. Table 1 of Davidge et al. 2004). The  $Z = 0.008$  models are adopted as the baseline for subsequent discussion and comparison, although the reader is reminded that the AGB age estimates depend on the adopted metallicity.

The  $Z = 0.008$  isochrones predict that the majority of stars in the  $(i', r' - i')$  CMD have ages between  $\log(t) = 8.0$  and  $9.0$ . However, there is also a modest population of objects with  $(r' - i') \sim -0.3$  that have photometric properties that are consistent with them being main sequence stars with ages  $\log(t) \sim 7.5 - 8.0$ . These stars have brightnesses where contamination from blends of fainter stars becomes significant (§2.3), and so the detection of moderately bright main sequence stars in these data should be considered to

be preliminary. Still, evidence to support the main sequence interpretation comes from the presence of possible red supergiants (RSGs) that are located on or near isochrones that pass through the region of the CMDs that is occupied by the candidate main sequence stars.

The benefits of observing metal-rich AGB stars at wavelengths longward of  $1\mu\text{m}$  are clearly illustrated when comparing the isochrones in Figures 3 and 4. The models show that the AGB slumps over on the  $(i', r' - i')$  CMD, whereas the AGB is much closer to vertical on the  $(K, J - K)$  CMD, due to the diminished impact of line blanketing at longer wavelengths. In fact, the locus of peak  $M_K$  brightnesses defined by the  $\log(t) = 8.0, 8.5,$  and  $9.0$  isochrones roughly tracks the upper envelope of the AGB concentration on the  $(M_K, J - K)$  CMD. This being said, the isochrones only pass through the blue end of the AGB plume, and miss many red sources in M82. This situation does not change when the  $Z = 0.019$  models are considered. The inability to reproduce the full range of observed near-infrared colors may be due in part to incomplete – as opposed to incorrect – physics in the models. At least some of the objects with  $J - K \geq 1.5$  may be C stars (e.g. Davidge 2005), and the Girardi et al. (2002; 2004) models do not include these objects. It should also be kept in mind that this is the color range where the number density of background galaxies is highest (§3.1), so at least some of the red objects probably do not belong to M82.

### 3.3. An Overview of the LFs

The  $i'$  LFs of objects with  $r' - i'$  between 0 and 2 are shown in Figure 5. The LFs have been corrected for contamination from foreground stars and background galaxies by subtracting the LF of objects in control fields to the east and west of M82. The control fields subtend much larger areas than the M82 disk fields, and the control field LFs were scaled to account for these differences in area. The effects of crowding are clearly evident at the faint end of the 2 – 4 and 4 – 6 kpc LFs, where incompleteness causes the inflexion point in the number counts to set in  $\sim 0.5$  magnitude brighter than at larger radii. This is consistent with the results of the artificial star experiments (§2.3).

After correcting statistically for foreground and background objects, an excess number of stars remains in the 10 – 12 kpc interval, indicating that the stellar disk of M82 extends out to at least this radius. Therefore, while the CMDs that cover the 10 – 12 kpc intervals in Figures 1 and 2 do not show an obvious concentration of AGB stars, a modest number of stars that belong to M82 are present. The peak AGB  $i'$  magnitudes predicted for various ages from the  $Z = 0.008$  Girardi et al. (2004) models are indicated at the top of Figure 5. Caution should be exercised when using this calibration, as photometric variability smears the location of the AGB-tip. There are also uncertainties in the models, which only extend to

the onset of thermal pulses. These models also overestimate the number of AGB stars when compared with RGB stars, possibly indicating that mass loss rates have been underestimated (Williams et al. 2007). With these caveats in mind, there is evidence of a  $\log(t) = 8.1$  population in all distance intervals, indicating that much of the M82 disk formed stars during intermediate epochs. The objects with  $i' < 22$  in the  $i'$  LFs are RSGs that formed within the past  $\sim 0.1$  Gyr.

The  $K$  LFs of objects with H–K between 0 and 1 are shown in Figure 6. As with the  $i'$  LFs, the  $K$  LFs indicate that the stellar disk of M82 extends out to at least 12 kpc, and that intermediate age stars are present over a large fraction of the stellar disk. The number of stars per magnitude in the  $K$  and  $i'$  data differs because the AGB is distributed over a larger range of  $K$  magnitudes than  $i'$  magnitudes. The AGB-tip at 10 – 12 kpc in the  $K$  LF is consistent with an age  $\log(t) = 9.0$ , which is older than the AGB-tip brightnesses at smaller radii. While this points to a possible conflict with the  $i'$  LFs, where the AGB-tip brightness corresponds to  $\log(t) = 8.1$  at all radii, there are large uncertainties in the number counts at the bright end in the 10 – 12 kpc LFs in both filters, so the significance of any difference is low. The population of RSGs that is seen in the 2 – 6 kpc  $i'$  LFs appears to be missing in the  $K$  LFs. However, this is likely a consequence of the relative brightnesses of RSGs and AGB stars in the near-infrared, which is such that RSGs with ages  $> 60$  Myr are fainter in  $K$  than AGB-tip stars that have  $\log(t) < 9.0$ .

### 3.4. The Spatial Distribution of Stars in the Disk

Specific frequency (SF) measurements provide a means of quantifying the spatial distribution of stars. Following previous studies by the author, the SF is taken to be the number of objects in a given color interval that would be seen in an object with an integrated brightness  $M_K = -16$ . The total  $M_K$  in each spatial interval in M82 was calculated from the  $J$ –band light profile measured by Jarrett et al. (2003) from 2MASS data, which was extrapolated along an exponential profile to include the outermost regions of the disk. While  $K$ –band measurements are more sensitive to the stars that trace most of the stellar mass, the 2MASS  $K$ –band light profile does not extend to radii larger than  $\sim 8$  kpc in M82, and at large radii is much noisier than the  $J$ –band profile.  $M_K$  in each interval was calculated by assuming that  $J-K = 0.8$ , in agreement with 2MASS observations of M82 at intermediate radii.

The SFs of red stars in the MegaCam and WIRCam data are shown in Figures 7 and 8. The error bars show the uncertainties due to the number of objects in each magnitude interval. The dotted line is a power law that was fit to the mean SF measurements at intermediate brightnesses in the 4 – 10 kpc intervals, and this relation is shown in the figures

to provide a reference for annulus-to-annulus comparisons. The  $i'$  and  $K$  SF measurements agree with the mean relation throughout much of the disk. The one exception is in the 2 – 4 kpc interval, where  $SF_{i'}$  is lower than the mean relation when  $i' > 22$ . This is due to incompleteness in the MegaCam data in this crowded portion of the galaxy, and the  $SF_K$  measurements at the same radii agree with the mean trend. The comparisons in Figures 7 and 8 indicate that the AGB component throughout most of the disk of M82 is uniformly mixed with the main body of stars that dominate the integrated light.

Comparing the SFs of stars in M82 with those in other galaxies is of interest for probing the nature of M82 prior to the interactions with M81. The star-forming history of M82 can be explored in a purely empirical manner by comparing the SF measurements in Figures 7 and 8 with those in other galaxies. If the specific SFR in the outer disk of M82 was greatly elevated during intermediate epochs then the SF of AGB stars in M82 should be higher than in a ‘normal’ star-forming galaxy. The Sc galaxy NGC 2403 is adopted here as a benchmark ‘normal’ late-type spiral galaxy for this comparison, as it is in an isolated part of the M81 group (e.g. Karachentsev et al. 2002), has a stellar content that is similar to that of other late-type spirals (e.g. Davidge & Courteau 2002), and has moderately deep MegaCam and WIRCam observations (Davidge 2007).

The SF of stars in NGC 2403 were computed from the observations discussed by Davidge (2007) after applying the same selection criteria employed to reject objects with large photometric uncertainties in M82 (§2.3). The light profile of NGC 2403 measured from 2MASS data does not extend to large radii, and so the  $K$ –band surface brightnesses in NGC 2403 were computed from the  $r$ –band surface brightness profile that was ‘extended by hand’ by Kent (1987). A color  $V - K = 2.2$  was assumed, based on measurements of NGC 2403 at radii where the 2MASS and  $r$ –band light profiles overlap.

The SFs of stars in the outer disk of M82 and NGC 2403 are compared in Figure 9. The NGC 2403 SF measurements have been shifted faintward by 0.5 magnitudes as the distance modulus of NGC 2403 (Freedman & Madore 1988) is 0.5 mag lower than that of M82. As in Figures 7 and 8, the error bars show the uncertainties due to the number of objects in each magnitude interval. After correcting for differences in distance, the  $i'$  SFs of red stars in M82 and NGC 2403 are in reasonable agreement at  $i' = 23.0 - 23.5$ , which is where AGB-tip stars with ages  $\sim 0.3 - 0.6$  Gyr are found. As for the  $K$ –band data, the SF measurements of both galaxies agree at  $K = 19$ , which corresponds to the peak brightness of AGB stars with ages  $\sim 0.6$  Gyr. However, the NGC 2403  $SF_K$  curve falls below the M82 measurements at fainter magnitudes, suggesting that the specific SFRs of the outer disks of M82 and NGC 2403 may have differed  $> 1$  Gyr in the past, in the sense that M82 had more vigorous star-forming activity.

The situation is different when the SF measurements of NGC 2403 and M82 are compared at the bright end. The  $K$ -band SF measurements of NGC 2403 fall above those of M82 when  $K_{M82} < 19$ . While the large error bars indicate that caution should be exercised when drawing conclusions from the  $SF_{i'}$  comparisons alone, when  $i'_{M82} < 23$  there is a systematic tendency for the NGC 2403  $SF_{i'}$  measurements to fall above those of M82. These differences occur in the magnitude range that contain RSGs and the brightest AGB stars (Figure 3). Therefore, the comparisons in Figure 9 suggest that while star formation has continued in the outer disk of NGC 2403 during the past  $\sim 100$  Myr, the specific SFR has been lower in the outer disk of M82 during this same time period.

If the specific SFRs in the outer disks of NGC 2403 and M82 during the past few hundred Myr have been markedly different then this should be evident when their CMDs are compared. The  $(i', r' - i')$  CMDs of stars with galactocentric distances between 6 and 8 kpc in the disks of NGC 2403 and M82 are compared in Figure 10. As in Figure 9, the NGC 2403 measurements have been shifted faintward by 0.5 magnitude to adjust for the difference in distance. There are many more stars with  $R_{GC}$  between 6 and 8 kpc in NGC 2403 than in M82, and this complicates efforts to compare the CMDs. To account for this, the middle panel of Figure 10 shows the CMD of stars in the NGC 2403 6 - 8 kpc interval in small fields near the minor and major axes of NGC 2403 that together contain the same number of stars with  $i'_{M82}$  between 23.25 and 23.75 as in the 6 - 8 kpc interval in M82.

The CMDs of NGC 2403 and M82 in Figure 10 are very different. The M82 CMD lacks the plume of RSGs with  $r' - i'$  between 0.3 and 1.1 that dominates the NGC 2403 CMD when  $i'_{M82} < 23$  (i.e.  $M_{i'} < -5$ ). The isochrones in Figure 3 indicate that the RSG sequence in this magnitude range is dominated by stars that are younger than  $\sim 100$  Myr. The CMD of M82 also lacks the spray of bright blue main sequence stars with  $r' - i' < 0$  that is seen in the NGC 2403 CMD. This is also consistent with the outer disk of M82 lacking stars that formed during the past  $\sim 100$  Myr. In summary, while the comparisons in Figure 9 indicate that the specific SFRs in the outer disks of M82 and NGC 2403 may have been similar 0.1 - 1 Gyr in the past, the CMDs in Figure 10 indicate that during the past  $\sim 100$  Myr the specific SFR in the outer disk of M82 has been much lower than in NGC 2403.

#### 4. BRIGHT EXTRAPLANAR STARS AND CLUSTERS

The outflow from the star-forming regions in M82 injects hot gas into the extraplanar environment. Some of this gas appears to have cooled sufficiently to allow stars to form, as stars with ages  $\sim 50$  Myr are seen in M82 South (Davidge 2008). While M82 South appears to be the most obvious extraplanar stellar structure associated with M82 (§4.2), there may

be other, albeit less pronounced, collections of young extraplanar stars. In this section, a search is conducted for young and intermediate age stars in the extraplanar environment. A list of globular cluster candidates is also compiled.

#### 4.1. An Overview of the CMDs

The investigation is restricted to a 6.5 arcmin wide strip that extends perpendicular to the major axis of M82. Given that the stellar disk of M82 has been traced out to a galactocentric radius of *at least* 12 kpc (§3), and that the disk of M82 is inclined at 77 degrees, then disk stars will be present out to a projected distance along the minor axis of at least  $\sim 3$  kpc. Therefore, to reduce contamination from disk stars on the near and far sides of the M82 disk only projected minor axis distances,  $D_Z$ , in excess of 2.5 kpc are considered. An ellipticity of 0.68 (Jarrett et al. 2003) is assumed when sorting stars into  $D_Z$  intervals.

The  $(i', r' - i')$  and  $(z', r' - i')$  CMDs of the extraplanar regions of M82 are shown in Figure 11, while the corresponding  $(K, H - K)$  and  $(K, J - K)$  CMDs are shown in Figure 12. The CMDs that are closest to the disk plane are richly populated, with a conspicuous concentration of AGB stars. There is also a spray of bright red objects above the AGB, many of which are probably RSGs. Contamination from disk stars is greatest at  $D_Z = 3$  kpc, and so it is perhaps not surprising that the  $D_Z = 3$  kpc CMDs are similar to those in the outer disk of M82 (§3.1).

The number of stars that belong to M82 decreases as  $D_Z$  increases, and at  $D_Z = 7$  kpc contamination from relatively blue ( $H - K \sim 0.1$ ,  $J - K \sim 0.6$ ) foreground stars and relatively red ( $H - K \sim 0.9$ ,  $J - K \sim 1.6$ ) background galaxies dominate the infrared CMDs in Figure 12. Still, a concentration of AGB stars can be traced out to  $D_Z = 7$  kpc in Figures 11 and 12, while objects with colors and brightnesses that are consistent with them being RSGs are also seen out to  $D_Z = 7$  kpc in Figure 11. The presence of possible RSGs at this  $D_Z$  is perhaps not surprising given that RSGs are present in M82 South (Davidge 2008).

#### 4.2. Comparisons With Isochrones

The CMDs of objects with  $D_Z = 3$  and 5 kpc are compared with isochrones from Girardi et al. (2002; 2004) in Figure 13. Given that gas in M82 appears to have a solar metallicity (discussion in §3), then  $Z = 0.019$  models are shown in Figure 13. These models do a reasonable job of matching the red envelope of objects with  $M_{i'} > -5$  in the MegaCam data, although some of the reddest objects are probably background galaxies. It should be

recalled that the  $Z = 0.008$  and  $Z = 0.019$  isochrones predict ages for AGB stars that differ by  $\sim 0.5$  dex (§3).

There are objects in the  $(M_{i'}, r' - i')$  CMDs that have photometric properties that are consistent with those of main sequence stars with ages  $\leq 100$  Myr. These are likely real sources, as opposed to spurious blends of objects, for two reasons. First, the sequence of blue stars extends well above the  $i' = 24.5$  ( $M_{i'} = -3$ ) limit where the artificial star experiments suggest that blends occur in significant numbers (§2.3). Second, the region of the CMDs that contains RSGs of the same age as the candidate main sequence stars is well populated. Older objects are also present, as there are stars on the AGB that have an age  $\log(t) \leq 8.5$  on the  $(M_{i'}, r' - i')$  CMDs. Thus, it is concluded that the extraplanar regions of M82 contains stars (1) with ages  $< 100$  Myr, and (2) that span a range of ages.

### 4.3. An Overview of the LFs

The  $i'$  LFs of stars with  $r' - i'$  between 0 and 2 are shown in Figure 14, while the  $K$  LFs of stars with  $H - K$  between 0 and 1 are shown in Figure 15. The LFs were corrected for contamination from foreground stars and background galaxies by subtracting number counts from the control fields, which were scaled to match the counts expected in the area covered at each  $D_Z$ . There remains a significant number of stars at the faint end of the LFs in all  $D_Z$  intervals after applying this correction, quantitatively confirming the results from the CMDs in Figures 11 and 12 that intermediate age stars with ages  $\leq 1$  Gyr are seen in the extraplanar regions of M82.

The dashed lines in Figures 14 and 15 show the reference SF relations from Figures 7 and 8, which have been scaled to match the number of objects near the faint end of the extraplanar LFs. These fiducial relations are in reasonable agreement with the general trends defined by the extraplanar LFs. Still, there is an excess number of objects with  $K = 18.5 - 19.0$  in the  $D_Z = 7$  kpc interval when compared with the fiducial relation, and also near  $i' = 21$  in the  $D_Z = 6$  and 7 kpc intervals. These departures from the disk trend are due to RSGs in M82 South.

### 4.4. The Spatial Distribution of Extraplanar Sources

The numbers of objects in the  $i' = 23, 23.5,$  and  $24.0$  bins of Figure 14, which are the magnitude intervals that are dominated by bright AGB stars, indicate that the exponential scale length of extraplanar AGB stars along the minor axis is  $1.8 \pm 0.2$  kpc. This is comparable



to the scale lengths of stellar disks. The spatial distribution of sources with  $r' - i' < -0.2$  and  $i' < 25$ , which are notionally main sequence stars, and sources with  $r' - i'$  between 0 and 2, and  $i'$  between 24.5 and 23.0, which are candidate AGB stars and RSGs, are shown in Figure 16. It can be seen that the spatial distribution of sources is not equally distributed between the northern and southern portions of the galaxy.

There is a tendency for the blue objects to have higher densities close to the M82 disk, and there are significantly more blue objects to the south of M82 than to the north. Blue objects are seen out to  $\sim 7$  kpc, especially to the south of the main body of the galaxy. M82 South, which contains stars with an age  $\sim 50$  Myr (Davidge 2008), appears as only a modest collection of blue objects in Figure 16.

There are many more red sources than blue sources, making candidate AGB stars potentially more powerful probes of structure. The candidate AGB stars tend to occur along the minor axis in the outflow. M82 South is clearly visible in the distribution of red stars as the collection of objects near  $(x,y) = (2600,6000)$  in the co-ordinate system used in Figure 16. M82 South roughly defines the southern boundary of the concentration of AGB stars that are associated with the southern outflow. There are no other concentrations of AGB stars that are similar in density to M82 South; M82 South could be a unique object, or if similar structures formed earlier then they have since dispersed.

#### 4.5. Fossil Globular Clusters

If, as suggested by O’Connell & Manganò (1978), M82 was at one time a late-type disk galaxy then it also would have been accompanied by a modest entourage of globular clusters. The number of clusters that would have been present can be estimated by assuming that the SF of globular clusters in M82 was similar to that of other late-type galaxies. Given the current levels of star formation in M82, the total brightness of M82 is best compared with that of other galaxies in the near-infrared, where the signal is less sensitive to differences in stellar content and dust extinction. With a total brightness  $K = 4.7$  (Jarrett et al. 2003), then  $M_K \sim -23.3$  for M82. The Leitherer et al. (1999) STARBURST99 models suggest that even if a large fraction of the  $K$ -band light comes from recently formed stars, which is likely the case near the center of M82, then the  $K$  brightness will fade by no more than  $\sim 2$  mag over the next billion years. Thus, it is likely that  $M_K < -21.3$  for M82 in its pre-interaction state. The integrated brightness of the Sc galaxy NGC 2403 is  $M_K \sim -21.3$  (Jarrett et al. 2003), and it is accompanied by tens of globular clusters (e.g. discussion in Davidge 2007). Therefore, the progenitor of M82 then likely also had tens of old clusters if it was a late-type disk galaxy.

While some of the globular clusters associated with M82 may have been lost during the encounter with M81, a remnant fossil population might remain. Saito et al. (2005) discuss a combined imaging and spectroscopic survey for globular clusters within 3 arcmin of the center of M82. They find 40 objects with brightnesses and colors that fall within the range occupied by Galactic globular clusters, and a spectroscopic follow-up of a subset of these yielded 2 old globular clusters and 3 young clusters.

The ironclad identification of clusters outside of the area studied by Saito et al. (2005) will require spectroscopic information and high angular resolution images, but photometric data alone with sub-arcsec resolution can still be used to identify plausible globular cluster candidates. The WIRCam observations of M82 are of particular interest in this regard because they cover a large field of view, and metal-poor globular clusters have colors that are different from the vast majority of bright stars in galaxy disks. Following the procedure employed by Davidge (2007), candidate old globular clusters in the extraplanar regions of M82, as defined in §4.1, were identified based on their infrared colors, angular size, and appearance. More specifically, objects were identified that (1) have  $J - K \leq 1$ , and (2) are non-stellar, based on the DAOPHOT *sharp* parameter. The objects identified with these criteria were then inspected by eye to remove sources that are obvious spiral galaxies or blended stars. The crowded central regions of the galaxy, where the largest number of clusters may be located, was avoided as stellar blends and asterisms may masquerade as clusters in such an environment.

If the globular cluster LF (GCLF) of the progenitor galaxy was like that in M31 (Barmby, Huchra, & Brodie 2001) then the majority of globular clusters in M82 will have  $M_K$  between  $-12$  and  $-9$ , or  $K \sim 16 - 19$ , and should thus be bright enough to be detected in the WIRCam data. Five globular cluster candidates were found, and their locations, brightnesses, colors, and de-convolved angular sizes, where the latter assumes that the seeing disk and light distribution of the candidate clusters are Gaussians, are summarized in Table 1. The astrometry is based on the co-ordinates of stars detected by 2MASS close to the cluster candidates. All of the candidate clusters are to the south of M82, and three are within 5 arcmin of each other at a projected distance of  $\sim 17$  kpc (15 arcmin) from the disk plane.

The intrinsic angular sizes of the cluster candidates corresponds to  $7 - 13$  parsecs at the distance of M82. This places these objects at the upper end of the half-light radius distribution of old Galactic halo globular clusters, but well within the range of half light radii of objects identified as young halo clusters by MacKey & van den Bergh (2005). The criterion used by MacKey & van den Bergh (2005) to distinguish between old and young halo clusters is horizontal branch morphology, and the young halo clusters are only a few Gyr younger than the oldest halo clusters. Thus, despite being labelled as ‘young’ they still

formed during relatively early epochs.

## 5. DISCUSSION AND SUMMARY

Wide field CFHT MegaCam and WIRCam images with sub-arcsec angular resolution have been used to probe (1) the spatial extent and stellar content of the M82 stellar disk, and (2) the stellar content in the extraplanar regions of M82. Stars in the disk of M82 are traced out to major axis distances of 12 kpc, which is comparable to the spatial extents of stellar disks in other nearby late-type spirals. The number of bright AGB stars per unit surface brightness (the ‘specific frequency’ – SF) in the outer disks of M82 and the Sc galaxy NGC 2403 are similar. To the extent that red and infrared surface brightness serve as a proxy for projected stellar mass density, then this suggests that the specific SFR in the outer disks of these galaxies were similar during intermediate epochs. That the radial size of the stellar disk and the SF of bright AGB stars in M82 are similar to those in NGC 2403 is consistent with M82 having been a gas-rich late-type disk galaxy prior to encountering M81. However, the SF of RSGs in the outer disk of M82 is much lower than in NGC 2403, suggesting that the star-forming histories of these galaxies diverged within the past  $\sim 0.1$  Gyr. This is probably a consequence of the interaction with M81, which disrupted the ISM of M82.

The interaction with M81 has also had a major impact on the extraplanar regions of M82. Feedback from the star-forming regions ejects material out of the disk plane, while the tidal interactions with M81 may also have pulled some of the ISM from the disk of M82, and deposited it around the galaxy. Given the presence of extraplanar gas, it is interesting that a mixture of bright main sequence stars, RSGs, and AGB stars that extend up to projected distances of at least  $\sim 7$  kpc above the disk plane are seen in the CFHT data. The exponential scale height of bright AGB stars is  $1.8 \pm 0.2$  kpc, which is considerably larger than what is traditionally associated with disk thickness. The photometric properties of the most evolved extraplanar RSG and AGB stars are consistent with them being at least moderately metal-rich, indicating that they formed from material that likely came from a disk, as opposed to a chemically immature environment. There are also five objects that have photometric and structural properties that are consistent with them being metal-poor globular clusters. Given that (1) stars evolving on the RSG and AGB sequences have different ages, and (2) the progenitor of M82 presumably contained a modestly populated classical (e.g. old and metal-poor) halo, of which globular clusters are the brightest tracers, then the extraplanar regions of M82 contain stars spanning a broad range of ages and metallicities.

### 5.1. A Spatially Extended Stellar Disk in M82

Individual bright AGB stars have been detected in the CFHT images out to 12 kpc along the major axis of M82. The SF of AGB stars between major axis distances of 4 and 12 kpc is constant, indicating that the AGB stars (1) belong to the disk, and (2) are uniformly mixed throughout the disk. Therefore, the stellar disk of M82 extends to much larger radii than sampled by, for example, 2MASS data, which traces the exponential light profile of M82 out to 350 arcsec ( $\sim 6.6$  kpc) (Jarrett et al. 2003).

The stellar disk of M82 almost certainly extends to distances  $> 12$  kpc. Unfortunately, lacking the spectroscopic information that would be helpful to distinguish between stars and galaxies, contamination from background galaxies frustrates efforts to push the detection of AGB stars to larger radii. This being said, the linear size of the M82 stellar disk as mapped with the CFHT data is at the small end of what is seen in other nearby late-type spirals that are at comparable distances and have been investigated using the same instrumentation. The stellar disk of NGC 2403 has been traced out to  $\sim 14$  kpc (Davidge 2007), while in NGC 247 the stellar disk extends to at least  $\sim 18$  kpc (Davidge 2006). However, when gauged in terms of disk scale length, the M82 stellar disk is relatively large. With an exponential scale length of  $\sim 0.9$  kpc (Mayya et al. 2005), then AGB stars in M82 are seen out to 13 scale lengths. For comparison, stars in NGC 247 and NGC 2403 are traced out to  $\sim 7$  scale lengths (Davidge 2006; 2007).

Mayya et al. (2005) trace spiral structure in near-infrared images of M82 out to  $\sim 2$  arcmin, or  $\sim 3$  kpc. Even though the stellar disk of M82 extends out to much larger radii (e.g. §3.1), spiral structure may not be expected in stellar light at distances larger than that found by Mayya et al (2005). The random motions imparted to stars as they encounter other objects in the disk cause them to diffuse from their places of birth, and spiral structure becomes increasingly blurred as the spatial distribution of stars with progressively larger ages are considered. Davidge (2007) found that the brightest main sequence stars in NGC 2403, which have ages  $\leq 10$  Myr, are excellent tracers of spiral structure, whereas RSGs with ages  $\sim 50$  Myr are not. Given that stars with ages of  $\sim 10$  Myr are rare outside of the central few kpc of M82 and that the brightest main sequence stars in the outer disk likely have ages approaching 100 Myr, then stellar light will not trace spiral arms outside of the inner few kpc of M82.

The time since the interaction between M81 and M82 is comparable to the crossing time of the M82 disk, and so large-scale signatures of tidal disturbances in the stellar disk might still be evident if they were ever present, and none are seen. That the disk of M82 extends out to many scale lengths and that the distribution of AGB stars does not show warping out of the disk plane suggests that the outer stellar disk was not greatly disrupted.

This is perhaps surprising given that Yun, Ho, & Lo (1993) find that the M82 gas disk is warped, while Yun et al. (1994) conclude that M82 likely harboured a large HI disk prior to interacting with M81, but that much of this gas has now been lost. There are a number of probable tidal structures near M81 and its companions, and at least some of these may have formed from gas that originated in M82. Indeed, simulations suggest that it is gas, rather than stars or dark matter, that is the key ingredient for the formation of long-lived tidal structures (Wetzstein, Naab, & Burkert 2007).

The large-scale behaviour of gas in and around the M82 disk is broadly consistent with model predictions. Brouillet et al. (1992) modelled the interactions between M81, M82, and NGC 3077, and reproduced the gaseous features that link these galaxies. However, these models assume that the disk of M82 was not greatly disturbed, whereas the distribution of HI and molecular material at the present day indicates that this is not the case. Still, the depleted ISM in M82 is concordant with models that demonstrate the fragility of disks during galaxy-galaxy encounters (e.g. Barnes 1992). Struck (1997) investigated models in which galaxies of unequal size, consisting of gas disks and rigid halos, collide. These simulations predict that the gas disks of both galaxies are drastically affected. Tidal forces cause the disk of the larger galaxy to expand, and a gas ring may form around this galaxy. A gas bridge, consisting mainly of material from the smaller galaxy, connects the two galaxies, while the gas that remains in the smaller galaxy contracts in size. The contraction of the gas disk of the smaller galaxy is consistent with the evidence that tidal interactions trigger the inward flow of disk gas (e.g. Iono et al. 2004; Kewley et al. 2006), which fuels centrally concentrated star-forming activity.

## 5.2. The Stellar Content of the Outer Disk

### 5.2.1. *A Recent Decline in the SFR in the Outer Disk of M82*

One motivation for studying nearby galaxies is that it is possible to resolve individual stars in areas that have also been studied spectroscopically. Mayya et al (2006) found that the spectrum of the M82 disk in the 1 – 3 kpc interval could be matched by that of a simple stellar system with an age  $\sim 0.5$  Gyr. Ostensibly, this might suggest the star-forming history of the M82 disk during intermediate epochs was spectacular. However, this is a luminosity-weighted age, that is skewed by the low M/L ratios of intermediate age stars. In §3.3 it is shown that the SF of AGB stars with ages  $\sim 0.5$  Gyr at large radii in M82 is similar to that in the outer regions of NGC 2403. The Sc galaxy NGC 2403 is relatively isolated, and is well removed from M81 and its companions (Karachentsev et al 2002). Thus, it is reasonable to assume that it has evolved in comparative isolation. To the extent that

NGC 2403 is a representative ‘normal’ late-type spiral galaxy, then this purely empirical comparison suggests that the specific SFR in M82  $\sim 0.5$  Gyr in the past was not markedly different from that in other late-type spiral galaxies. Given that the SFR in galaxy disks is likely to be roughly constant with time, then spectra of these objects should contain Balmer absorption features that are consistent with a population that formed within the past 1 Gyr that comprises  $\sim 10\%$  by mass of the stellar content. The visible light spectrum will then be that of an intermediate age population (e.g. Serra & Trager 2007), in agreement with that observed by Mayya et al. (2006) in M82.

The comparisons with NGC 2403 indicate that the outer disk of M82 is deficient in bright RSGs and main sequence stars. The relative paucity of RSGs in the outer disk of M82 suggests that the SFR dropped with respect to that in NGC 2403 within the past  $\sim 0.1$  Gyr. Given that other indicators suggest that M81 and M82 interacted at least 0.2 Gyr in the past, then it appears that star formation continued in the outer disk of M82 for a significant period of time after the interaction. Still, given the evidence that the ISM of M82 was affected by the interaction with M81 then it seems reasonable to conclude that the decline in the SFR 0.1 Gyr in the past is probably somehow linked to the interaction with M81.

The reader is cautioned that as highly evolved, relatively rare objects, RSGs are not an optimum probe of star-forming history. Observations of stars at the main sequence turn-off (MSTO) in the outer disk of M82 will provide a more reliable chronometer for determining when the SFR in the outer disk of M82 declined, and so the 0.1 Gyr age estimated for the drop in the SFR should be considered to be preliminary. The MSTO in the outer disk of M82 will occur near  $M_V \sim -2$  (i.e.  $V \sim 26$ ) if the SFR dropped 0.1 Gyr in the past.

### 5.2.2. Sources of Uncertainty in the Age Scale

There are various sources of uncertainty in the ages estimated in this paper. Uncertainties in the metallicities of the stars being investigated affects the age estimates. In §3 it was shown that the ages estimated for AGB stars from the  $Z = 0.008$  and  $Z = 0.019$  isochrones differ by  $\sim 0.5$  dex. Internal reddening is another possible source of uncertainty. It is likely that most of the dust at the present day is concentrated in the star forming regions near the center of M82. This being said, if the mean internal extinction measured for the central regions of the galaxy holds for the entire disk then the impact on ages is not great as long as the distance to M82 computed from RGB-tip measurements is also corrected for this reddening. Finally, the use of AGB stars as chronometers introduces uncertainties due to (1) the complicated model physics of highly evolved stars, (2) photometric variability, and (3)

stochastic effects due to the short evolutionary timescales of stars near the AGB-tip. The first of these can be mitigated somewhat by making direct comparisons between galaxies, as in §3.

Crowding also complicates efforts to probe the brightest stars in nearby galaxies, as blends of faint stars may appear as objects that skew age estimates to younger values. To reduce the impact of crowding, only stars that (1) are well outside of the crowded central regions of the galaxy and (2) are at brightnesses that the artificial star experiments indicate are not significantly contaminated by blends, have been considered in this study. The excellent annulus-to-annulus agreement in the SF measurements suggests strongly that crowding is not an issue when  $R_{GC} > 4$  kpc, and this is consistent with predictions from artificial star experiments.

A comparison of the properties of AGB stars from the MegaCam and WIRCam datasets can be used to test the claim that blending is not significant among the brightest AGB stars. This is because crowding has a very different impact on the brightest red stars at visible and near-infrared wavelengths, due largely to the wavelength-dependence of line blanketing. As the impact of line blanketing drops with increasing wavelength, there is increased contrast between red AGB stars and stars on the RGB, with the result that at infrared wavelengths there is a lower fraction of blends between RGB stars that may masquerade as bright AGB stars than at visible wavelengths.

If blending significantly affects the MegaCam observations more than the WIRCam observations then the  $M_{bol}$  LFs of AGB stars generated from the MegaCam data should contain stars that are brighter than those derived from the WIRCam data. To compare the LFs of the two datasets, the magnitudes of stars that have photometric properties that are consistent with M giants in the  $(i', r' - i')$  and  $(K, J - K)$  CMDs were converted into bolometric magnitudes. The comparison is restricted to M giants, as these are the stars that are common to both the MegaCam and WIRCam data. Bessell & Wood (1984) compute bolometric corrections (BCs) as functions of  $R - I$  and  $J - K$  colors, and these calibrations are adopted here.  $R - I$  colors were computed from the  $r' - i'$  colors using the transformation equations from Smith et al. (2002). Relations between  $T_{eff}$  and  $R - I$  and  $J - K$  were defined from data tabulated by Bessell (1979) and Bessell & Brett (1988).

The  $M_{bol}$  LFs of stars with  $\log(T_{eff})$  between 3.54 and 3.60 in two radial intervals are compared in Figure 17. The comparisons are affected by uncertainties in the BC and  $T_{eff}$  calibrations, and a large fraction of highly evolved AGB stars are expected to be photometrically variable. Still, the LFs constructed from the MegaCam and WIRCam datasets are in reasonable agreement, suggesting that blending does not affect the bright AGB stellar content in the  $(i', r' - i')$  CMDs.

### 5.3. Young and Intermediate-Age Stars in the Extraplanar Regions of M82

Stars with ages  $\log(t) \leq 9.0$  have been detected out to projected distances of  $\sim 7$  kpc above the M82 disk plane. Where did these stars form? The origin of these stars is discussed in this section.

Seth, Dalcanton, & de Jong (2005) investigate the vertical distribution of stars in a sample of nearby edge-on low mass disk galaxies. The vertical height of a star has an age dependence, in the sense that young stars are found closer to the disk than older stars. Seth et al. (2005) suggest that these stars belong to thick disks, that are populated by stars that leave the disk plane through dynamical heating, such as encounters with molecular clouds. Stars are detected up to 3.5 kpc above the disk plane, and Seth et al. conclude that the vertical scale height of thick disks in pure disk systems is larger than in the Galaxy. The young stars found in M82 extend to much larger distances off of the disk plane than those considered by Seth et al. (2005). Blue main sequence stars are also seen throughout the extraplanar regions of M82, whereas they should hug the disk plane if they were thick disk objects. While these arguments suggest that the majority of objects found in the extraplanar environment of M82 do not belong to a thick disk component, some stars in the  $D_z = 2.5\text{--}3.5$  kpc interval may be part of a thick disk like that seen in other disk systems.

A modest fraction of young disk stars will acquire high velocities due to dynamical processes. A fraction of OB stars in the Solar neighborhood have peculiar velocities  $\geq 30$  km  $\text{sec}^{-1}$ , and if these stars have space motions directed out of the disk plane then they could populate at least part of the extraplanar regions in the Milky-Way. Various mechanisms have been proposed to explain the high velocities of these stars, including ejection from close binary systems due to SN explosions, and dynamical ejection from young open clusters. Kiseleva et al. (1998) estimate that  $\sim 1\%$  of stars that form in small stellar systems will become high-velocity stars.

Could the youngest stars in the extraplanar regions of M82 be runaway objects? With a peculiar velocity of 30 km  $\text{sec}^{-1}$  then a star with an age of  $10^8$  years could traverse 3 kpc in its lifetime. Therefore, populating the extraplanar regions of M82 with stars that are younger than  $\sim 100$  Myr would require velocities in excess of 60 km  $\text{sec}^{-1}$ . Even if such stars were moving perpendicular to the disk plane, the maximum height that they could attain depends on the local gravitational potential, and stars ejected near the centers of galaxies at a given velocity will not reach the same distances above the disk as those in the outermost regions having the same velocity. While they may constitute some fraction of the young stellar component that is closest to the disk plane, stars ejected from the disk of M82 by dynamical processes probably can not populate the full extent of the extraplanar regions that have been probed in M82.



Given the evidence that the gas disk of M82 has been disrupted, then it is possible that some young and intermediate-age stars may have been pulled from the disk. If tidal forces populated the extraplanar regions of M82 then deeper observations should reveal two characteristics of the stellar content. First, tidal forces would have pulled a mix of young and old stars from the disk, so there should be an RGB component with a disk-like (i.e. moderately high) metallicity. Second, the spatial distribution of the stars pulled from the disk should not depend on age, and so the metal-rich RGB stars should be distributed with an exponential scale height that is the same as that of intermediate age AGB stars, which is 1.8 kpc. A major problem with the tidal origin model is that extraplanar stars with ages  $< 100$  Myr are hard to explain, as these objects formed well after M81 and M82 interacted.

It seems likely that some of the young and intermediate age stars in the extraplanar regions of M82 formed *in situ*. There are obvious difficulties forming stars in a hot outflow. Still, the formation of a shock where the outflow encounters gas or dust clouds surrounding M82, such as is thought to be occurring in the Cap (e.g. Lehnert et al. Strickland et al. 2004), could cool hot gas so that star formation can occur. de Mello et al. (2008) find star-forming regions in Arp’s Loop, which is an area of local HI concentration in the tidal debris trail between M81 and M82.

As discussed by Davidge (2008), the stars associated with M82 South likely do not form a bound structure, and tidal forces will likely disperse them in  $\sim 10^8 - 10^9$  years. de Mello et al. (2008) point out that the fate of the star-forming regions in Arp’s Loop is less clear. Still, if other structures like M82 South and those in the Arp Loop have formed in the past and have been disrupted then they may produce a diffusely-distributed population of youngish stars in the extraplanar regions of M82 and throughout the M81-M82 debris field.

The presence of relatively young stars may explain the extraplanar UV emission seen in M82. This emission is thought to come from UV radiation that is reflected from dust clouds. The source of the reflected light is not clear, although Hoopes et al. (2005) suggest that it may be the stellar continuum from the starburst. The FUV emission in the Hoopes et al. (2005) study is strongest along the minor axis to the south of the galaxy, and this is also where the largest number of candidate main sequence stars have been found (§4). Given that M82 South (1) is also a source of UV emission in the Hoopes et al. (2005) study, and (2) contains stars with ages of  $\sim 50$  Myr (Davidge 2008), then at least some of the FUV emission may come from main sequence stars in the extraplanar regions. In the particular case of M82 South, the strip of emission at visible wavelengths that defines the southern boundary of the stellar distribution may be reflected light from main sequence stars in M82 South.

We close by noting that the stellar content of the extraplanar regions of M82 may

provide clues for understanding the halos of other galaxies. It has been shown in this paper that stars in the extraplanar regions of M82 have diverse properties, with objects spanning ages from  $\log(t) \sim 7.5 - 9.0$ . Older stars are almost certainly present, but these are too faint to detect with the CFHT data. There are hints of an old extraplanar component in the form of globular clusters, although even if subsequent observations confirm that they are globular clusters they may still belong to M81.

Comparisons with isochrones indicate that the young and intermediate age stars in the extraplanar regions have a disk-like metallicity, which is higher than what might be associated with a classical halo. An observer a few Gyr in the future, well after the starburst activity has ceased, may see M82 as a disk galaxy with a marked spread in the metallicity and age of stars off of the disk plane. Such a dispersion in stellar content appears not to be rare in the outer regions of nearby spiral galaxies (Mouchine 2006), suggesting that interactions in the past may have had a role in populating the halos of many other galaxies.

It is a pleasure to thank the anonymous referee for comments that resulted in a greatly improved paper.

#	RA (2000.0)	Dec (2000.0)	$K$	$J - K$	FWHM (arcsec)
1	09:57:18	69:40:30	19.9	0.92	0.6
2	09:57:11	69:26:18	19.1	0.45	0.7
3	09:56:42	69:26:11	18.3	0.82	0.5
4	09:56:13	69:25:00	17.4	0.83	0.4
5	09:54:48	69:36:16	20.1	0.75	0.6

Table 1: Globular Cluster Candidates

## REFERENCES

- Barmby, P, Huchra, J. P., & Brodie, J. P. 2001, *AJ*, 121, 1482
- Barnes, J. E. 1992, *ApJ*, 393, 484
- Bessell, M. S. 1979, *PASP*, 91, 589
- Bessell, M. S., & Brett, J. M. 1988, *PASP*, 100, 1134
- Bessell, M. S., & Wood, P. R. 1984, *PASP*, 96, 247
- Bland-Hawthorn, J., Vlahic, M., Freeman, K. C., & Braine, B. T. 2005, *ApJ*, 629, 239
- Boulade, O, et al. 2003, *Proc. SPIE*, 4841, 72
- Boyce, P. J. et al., 2001, *ApJ*, 560, L127
- Brouillet, N., Baudry, A., Combes, F., Kaufman, M., & Bash, F. 1991, *A&A*, 242, 35
- Bullock, J. S., & Johnston, K. V. 2005, 635, 931
- Burstein, D., & Heiles, C. 1982, *AJ*, 87, 1165
- Cowie, L. L., Songaila, A., Hu, E. M., & Cohen, J. G. 1996, *AJ*, 112, 839
- Davidge, T. J. 2005, *AJ*, 130, 2087
- Davidge, T. J. 2006, *ApJ*, 641, 822
- Davidge, T. J. 2007, *ApJ*, 664, 820
- Davidge, T. J. 2008, *ApJ*, 678, L85
- Davidge, T. J., & Courteau, S. 2002, *AJ*, 123, 1438
- Davidge, T. J., Stoesz, J., Rigaut, F., Veran, J-P, & Herriot, G. 2004, *PASP*, 116, 1
- de Grijs, R., O’Connell, R. W., & Gallagher, J. S. III 2001, *AJ*, 121, 768
- de Mello, D. F., Smith, L. J., Sabbi, E., Gallagher, J. S., Mountain, M., & Harbeck, D. R. 2008, *AJ*, 135, 548
- Devine, D., & Bally, J. 1999, *ApJ*, 510, 197
- Forster Schreiber, N. M., Genzel, R., Lutz, D., & Sternberg, A. 2003, *ApJ*, 599, 193
- Freedman, W. L., & Madore, B. F. 1988, *ApJ*, 332, L63
- Gallagher, J. S. III, & Smith, L. J. 1999, *MNRAS*, 304, 540
- Girardi, L., Bertelli, G., Bressan, A., Chiosi, C., Groenewegen, M. A. T., Marigo, P., Salasnich, B., & Weiss, A. 2002, *A&A*, 391, 195
- Girardi, L., Grebel, E. K., Odenkirchen, M., & Chiosi, C. 2004, *A&A*, 422, 205

- Greve, A., Wills, K. A., Neininger, N., & Pedlar, A. 2002, *A&A*, 383, 56
- Hoopes, C. G. et al. 2005, *ApJ*, 619, L99
- Iono, D., Yun, M. S., & Mihos, C. 2004, *ApJ*, 616, 199
- Jarrett, T. H., Chester, T., Cutri, R., Schneider, S., & Huchra, J. P. 2003, *AJ*, 125, 525
- Karachentsev, I. D. et al. 2002, *A&A*, 383, 125
- Kazantzidis, S., Bullock, J. S., Zentner, A. R., Kravtsov, A. V., & Moustakas, L. A. 2007, astro-ph 07081949
- Kent, S. M. 1987, *AJ*, 93, 816
- Kewley, L. J., Geller, M. J., & Barton, E. J. 2006, *AJ*, 131, 2004
- Kiseleva, L. G., Colin, J., Dauphole, B., & Eggleton, P. 1998, *MNRAS*, 301, 759
- Larson, R. B., & Tinsley, B. M. 1978, *ApJ*, 219, 46
- Lehnert, M. D., Heckman, T. M., & Weaver, K. A. 1999, *ApJ*, 523, 575
- Leitherer, C. et al. 1999, *ApJS*, 123, 3
- Mackey, A. D., & van den Bergh, S. 2005, *MNRAS*, 360, 631
- Makarova, L. N., et al. 2002, *A&A*, 396, 473
- Mannucci, F., Basile, F., Poggianti, B. M., Cimatti, A., Daddi, E., Pozzetti, L., & Vanzi, L. 2001, *MNRAS*, 326, 745
- Martin, C. L. 1997, *ApJ*, 491, 561
- Mayer, L, et al. 2001, *ApJ*, 559, 754
- Mayya, Y. D., Carrasco, L., & Luna, A. 2005, *ApJ*, 628, L33
- Mayya, Y. D., Bressan, A., Carrasco, L., & Hernandez-Martinez, L. 2006, *ApJ*, 649, 172
- McKeith, C. D., Castles, J., Greve, A., & Downes, D. 1993, *A&A*, 272, 98
- Mouchine, M. 2006, *ApJ*, 652, 277
- O’Connell, R. W., & Manganano, J. J. 1978, *ApJ*, 221, 62
- O’Connell, R. W., Gallagher, J. S. III, Hunter, D. A., & Colley, W. N. 1995, *ApJ*, 446, L10
- Origlia, L., Ranalli, P., Comastri, A., & Maiolino, R. 2004, *ApJ*, 606, 862
- Parmentier, G., de Grijs, R., & Gilmore, G. 2003, *MNRAS*, 342, 208
- Puget, P., et al. 2004, *Proc. SPIE*, 5492, 978
- Saito, Y., et al. 2005, *ApJ*, 621, 750
- Sakai, S., & Madore, B. F. 1999, *ApJ*, 526, 599

- Sakai, S., & Madore, B. F. 2001, *ApJ*, 555, 280
- Schlegel, D. J., Finkbeiner, D. P., & Davis, M. 1998, *ApJ*, 500, 525
- Serra, P., & Trager, S. C. 2007, *MNRAS*, 374, 769
- Seth, A. C., Dalcanton, J. J., & de Jong, R. S. 2005, *AJ*, 130, 1174
- Smith, L. J., Westmoquette, M. S., Gallagher, J. S. III, O’Connell, R. W., Rosario, D. J., & de Grijs, R. 2006, *MNRAS*, 370, 513
- Smith, J. A., et al. 2002, *AJ*, 123, 2121
- Sofue, Y. 1998, *PASJ*, 50, 277
- Sofue, Y., Reuter, H-P, Krause, M., Wielebinski, R., & Nakai, N. 1992, *ApJ*, 395, 126
- Springel, S., & Hernquist, L. 2005, *ApJ*, 622, L9
- Stetson, P. B. 1987, *PASP*, 99, 191
- Stetson, P. B., & Harris, W. E. 1988, *AJ*, 96, 909
- Strickland, D. K., Heckman, T. M., Colbert, E. J. M., Hoopes, C. G., & Weaver, K. A. 2004, *ApJS*, 151, 193
- Struck, C. 1997, *ApJS*, 113, 269
- Sun, W.-H. et al. 2005, *ApJ*, 630, L133
- Walter, F., Weiss, A., & Scoville, N. 2002, *ApJ*, 580, L21
- Wetzstein, M., Naab, T., & Burkert, A., *MNRAS*, 375, 805
- Williams, B. F., et al. 2007, *ApJ*, 656, 756
- Wills, K. A., Das, M., Pedlar, A., Muxlow, T. W. B., & Robinson, T. G. 2000, *MNRAS*, 316, 33
- Yun, M. S., Ho, P. T. P., & Lo, K. Y. 1993, *ApJ*, 411, L17
- Yun, M. S., Ho, P. T. P., & Lo, K. Y. 1994, *Nature*, 372, 530

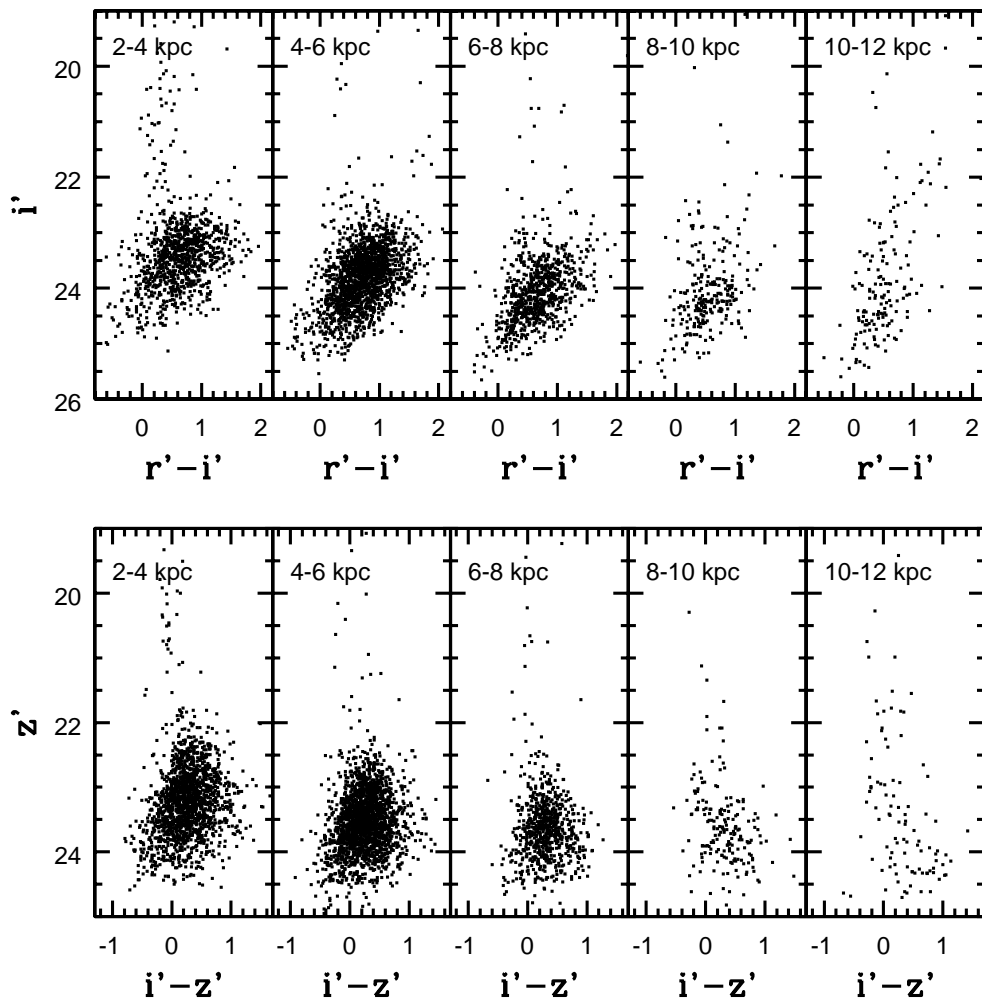


Fig. 1.— The  $(i', r' - i')$  and  $(z', i' - z')$  CMDs of stars within  $\pm 65$  arcsec of the major axis of M82. The concentration of objects in the lower half of the CMDs is made up of bright AGB stars in M82. These objects can be traced out to at least  $R_{GC} \sim 12$  kpc in M82.

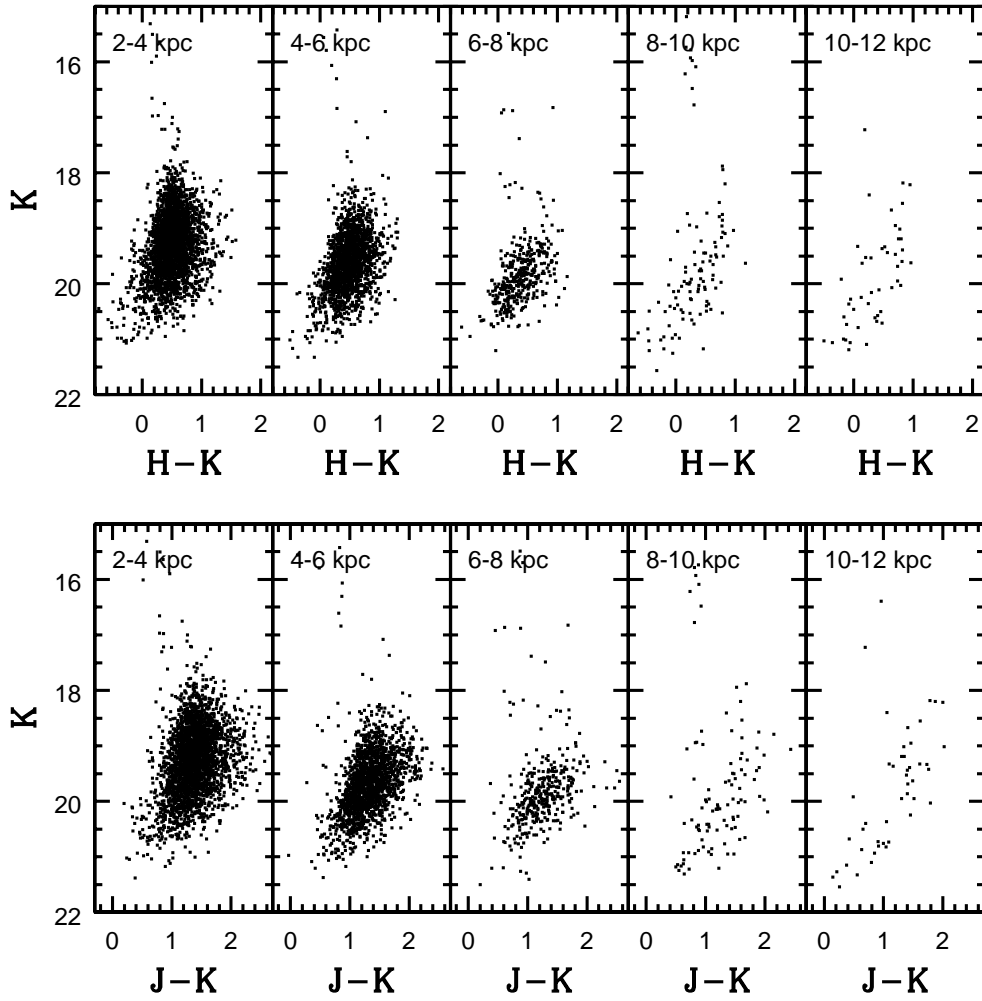


Fig. 2.— The same as Figure 1, but showing the  $(K, H - K)$  and  $(K, J - K)$  CMDs.



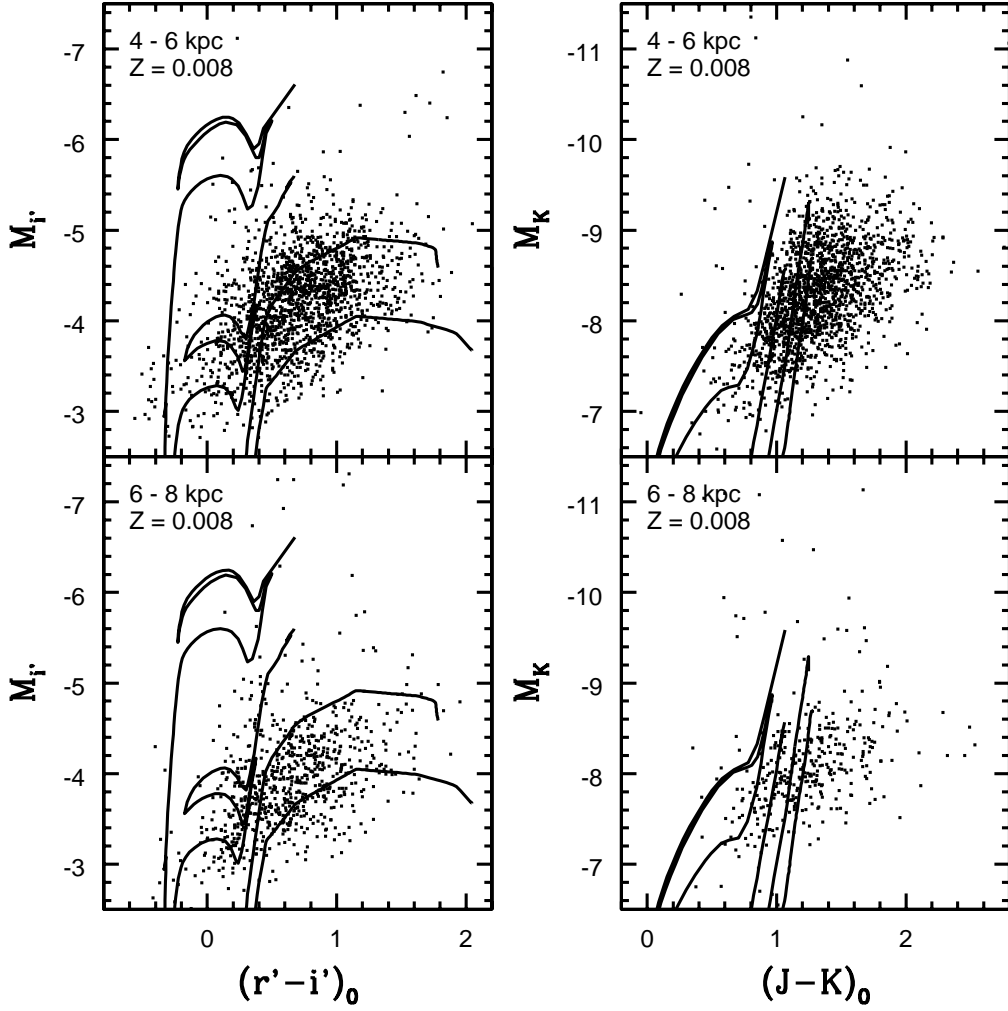


Fig. 3.— The CMDs of the 4 – 6 kpc and 6 – 8 kpc intervals in the M82 disk are compared with  $Z = 0.008$  isochrones from Girardi et al. (2002; 2004). The isochrones have  $\log(t_{yr}) = 7.5, 8.0, 8.5,$  and  $9.0$ . A distance modulus  $\mu_0 = 27.95$  has been assumed, with  $A_B = 0.12$  magnitude.

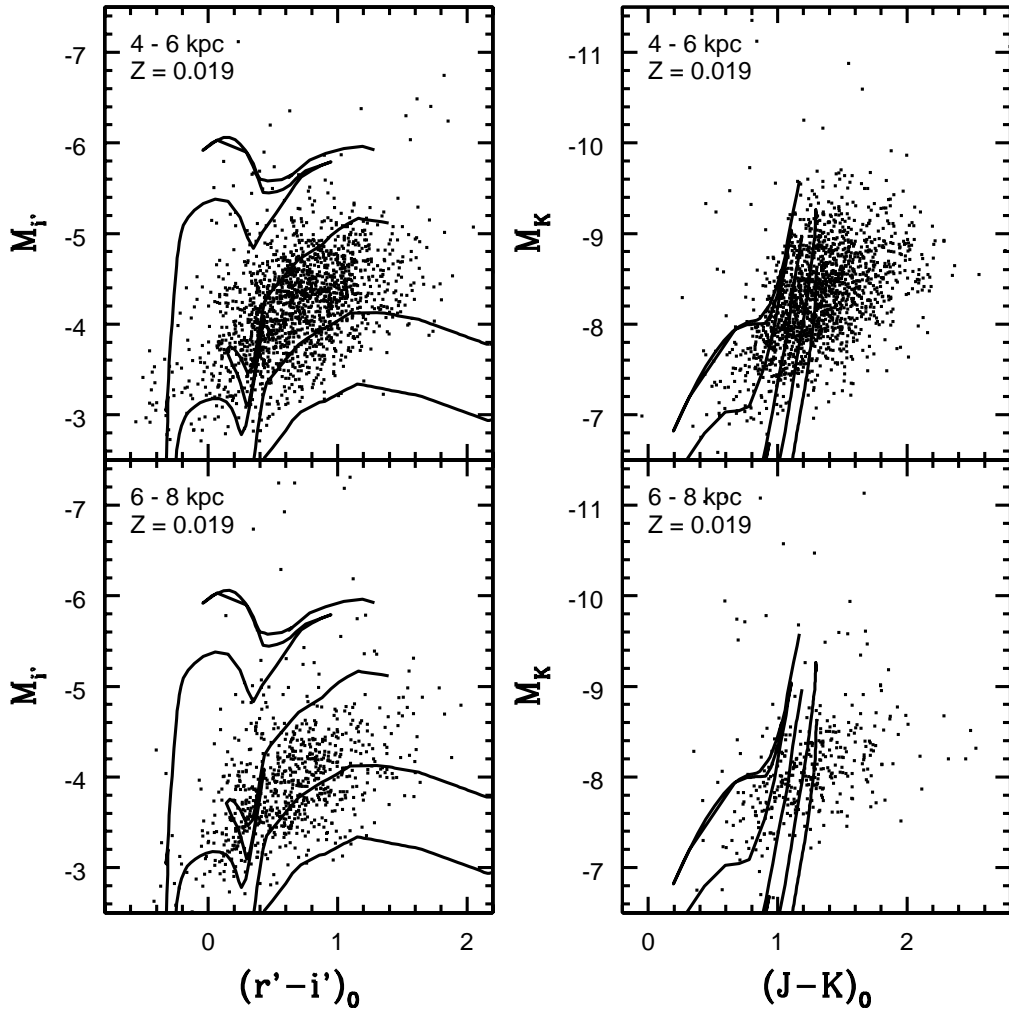


Fig. 4.— The same as Figure 3, but with  $Z = 0.019$  isochrones.

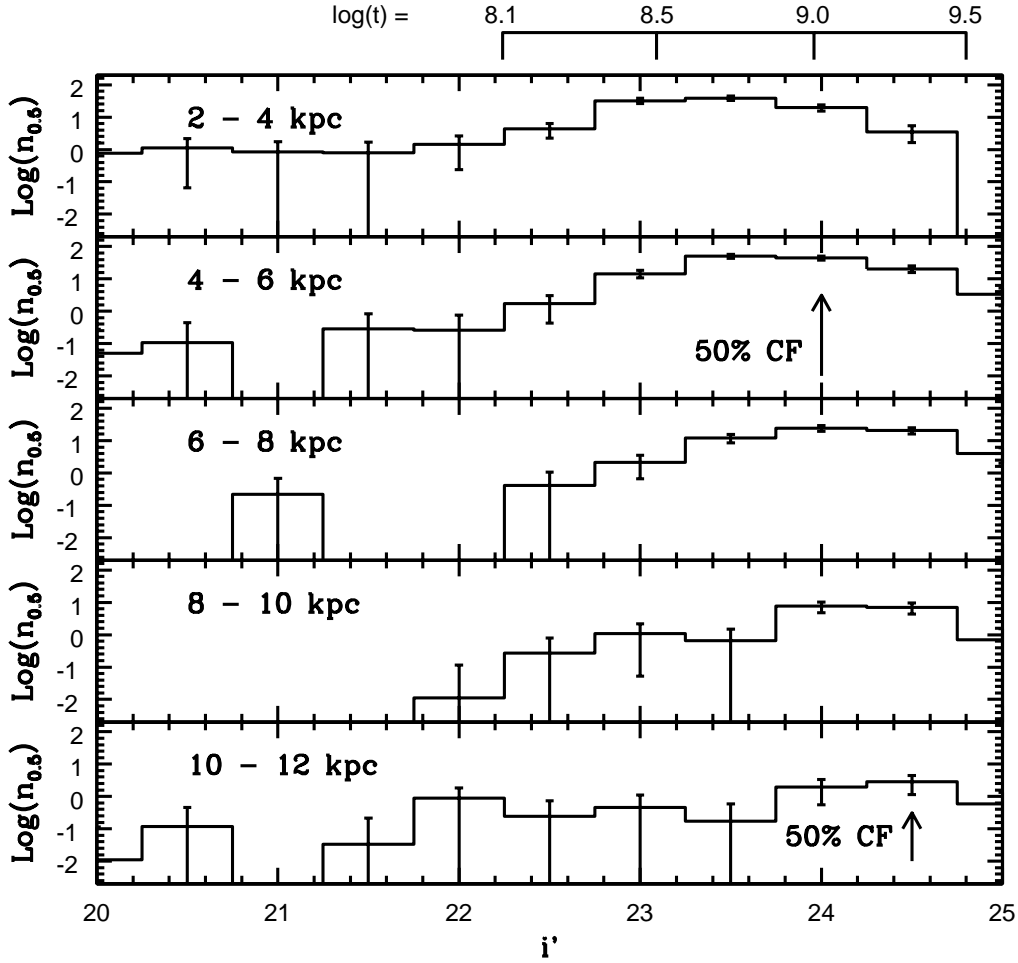


Fig. 5.— The  $i'$  LFs of stars in the M82 disk.  $n_{0.5}$  is the number of stars with  $r' - i'$  between 0 and 2 per  $0.5 i'$  magnitude per  $\text{arcmin}^2$ . The LFs have been corrected for contamination from foreground stars and background galaxies by subtracting the LF of control fields, scaled to account for the areal coverage in each radial interval. The magnitude at which the star counts have a 50% completeness fraction (50% CF) is indicated for the 4 – 6 and 10 – 12 kpc intervals. The peak AGB brightnesses predicted by the  $Z = 0.008$  Girardi et al. (2004) models for various ages are shown at the top of the figure.

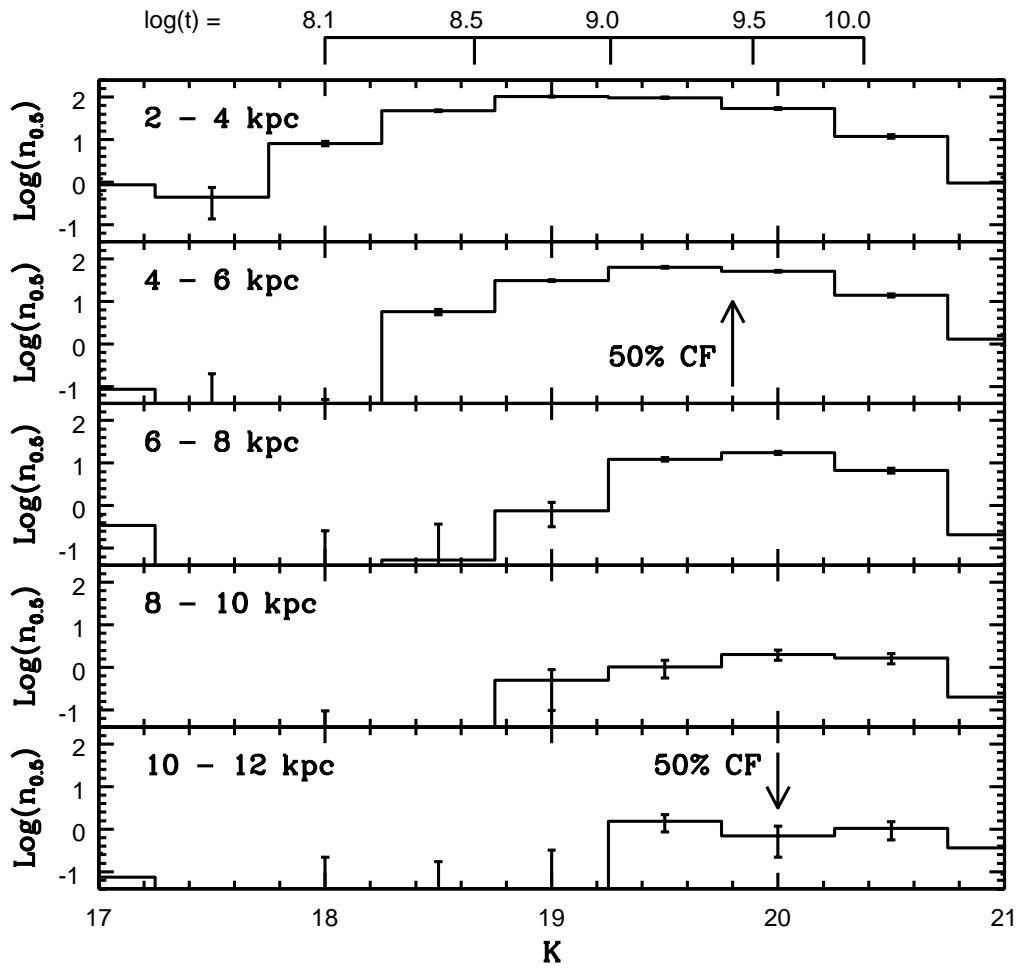


Fig. 6.— The same as Figure 5, but showing  $K$  LFs. The age calibration is based on the peak AGB brightnesses in the  $Z = 0.008$  Girardi et al. (2002) models.

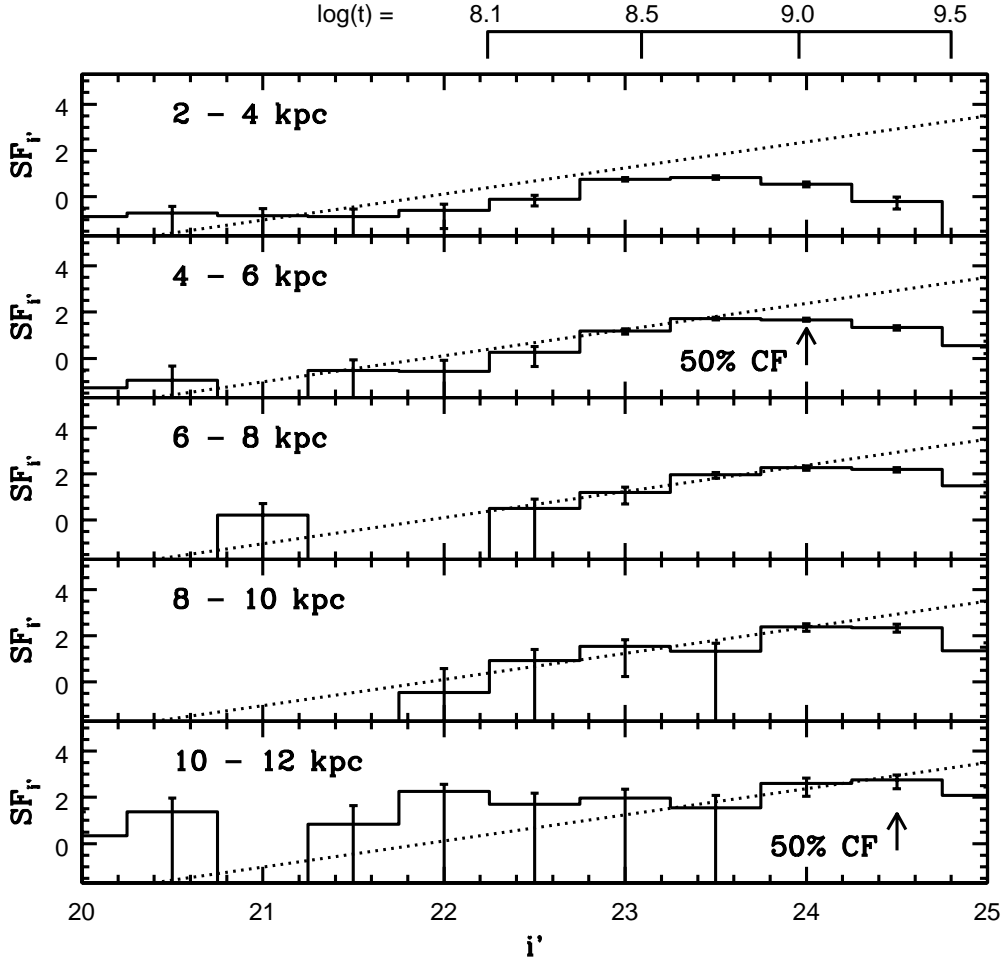


Fig. 7.— The specific frequency (SF) of stars measured from the MegaCam data.  $SF_{i'}$  is the number of stars with  $r' - i'$  between 0 and 2 per 0.5  $i'$  mag, scaled to match that in a system with a total magnitude  $M_K = -16$ . The dashed line shows the mean  $SF_{i'}$  relation at intermediate brightnesses for stars with  $R_{GC}$  between 4 and 10 kpc. The magnitude at which the star counts have a 50% completeness fraction (50% CF) is indicated for the 4 – 6 and 10 – 12 kpc intervals. The peak AGB brightnesses predicted by the  $Z = 0.008$  Girardi et al. (2004) models are shown at the top of the figure.

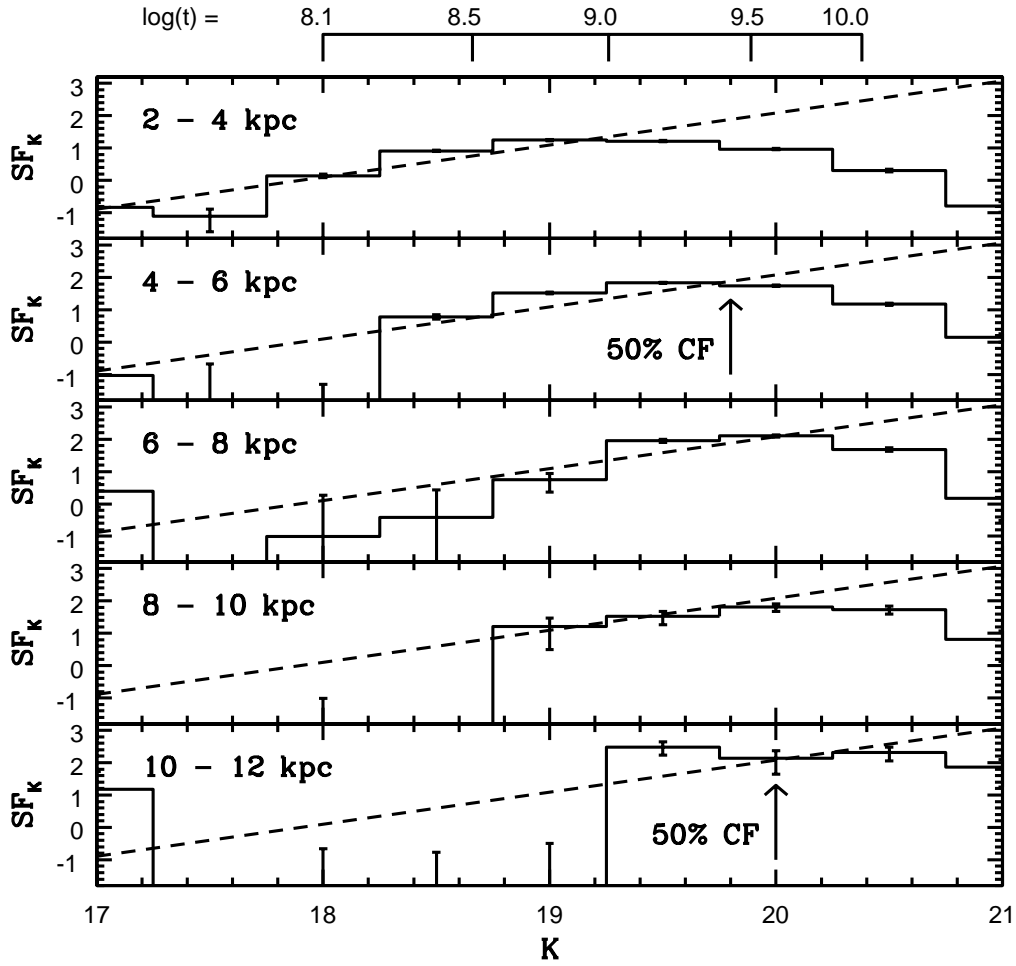


Fig. 8.— The same as Figure 7, but showing the SF of stars measured from the WIRCam data.  $SF_K$  is the number of stars with  $H - K$  between 0 and 1 per 0.5  $K$  mag, scaled to a system with a total integrated magnitude  $M_K = -16$ .

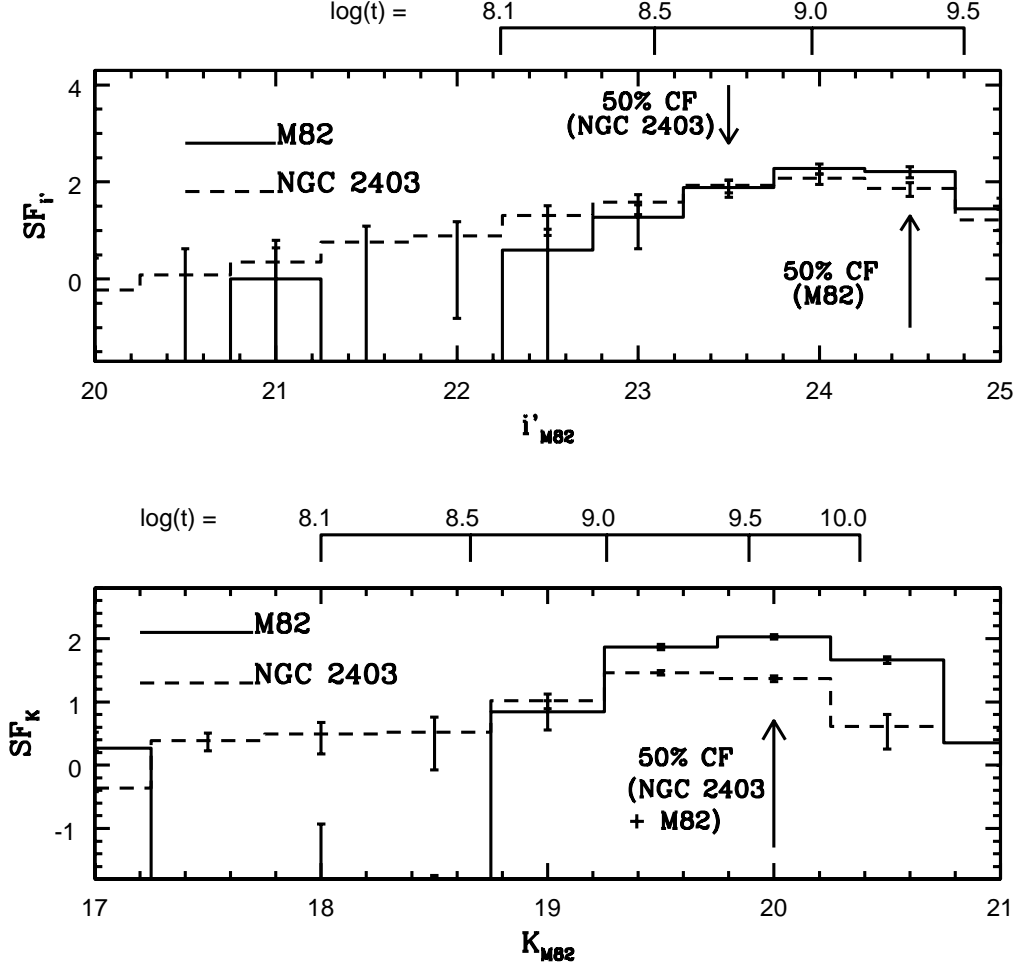


Fig. 9.— The SFs of stars in the outer disks of M82 (solid lines) and NGC 2403 (dashed lines).  $SF_{i'}$  and  $SF_K$  are defined in Figures 7 and 8. The M82 SF measurements use stars with  $R_{GC}$  between 6 and 10 kpc, while the NGC 2403 measurements include stars with  $R_{GC}$  between 6 and 12 kpc.  $i'_{M82}$  and  $K_{M82}$  are the brightnesses that would be measured at the distance modulus of M82, and the age calibration at the top of each panel shows the peak AGB brightnesses from the  $Z = 0.008$  Girardi et al. (2002; 2004) models. The magnitude at which the completeness fraction is 50% (50% CF) is indicated for each galaxy. Note the excellent agreement between the  $SF_{i'}$  curves of the two galaxies at brightnesses that correspond to the AGB-tip of systems with ages 0.3 – 0.6 Gyr. The  $SF_K$ 's also agree at  $K = 19$ , which corresponds to the AGB-tip brightness of a system with an age  $\sim 0.6$  Gyr. The comparisons in the top panel also suggests that the SF of RSGs in NGC 2403 is higher than in M82.

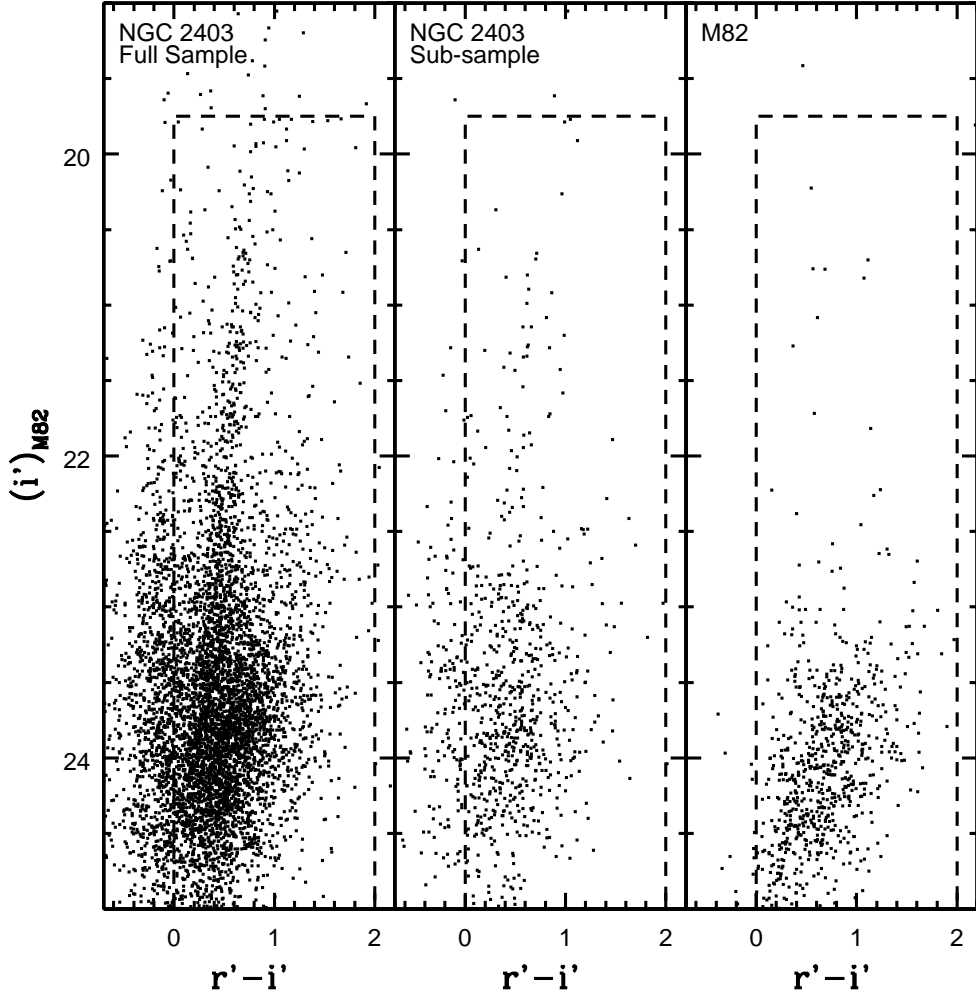


Fig. 10.— The  $(i', r' - i')$  CMDs of stars with  $R_{GC}$  between 6 and 8 kpc in NGC 2403 and M82.  $i'_{M82}$  is the brightness that a star would have if observed at the same distance as M82. The left and right hand panels show the CMDs of all stars in the 6 - 8 kpc intervals of both galaxies. The central panel shows the CMD of a sub-sample of stars from the left hand panel that are located in small fields near the minor and major axes of NGC 2403 and that together contain the same number of stars with  $i'_{M82}$  between 23.25 and 23.75 as in the M82 CMD. The dashed lines indicate the color intervals that were used to generate the star counts shown in Figure 9. The CMDs of NGC 2403 and M82 are very different, in that the M82 CMD lacks (1) the plume of RSGs with  $i' < 23$  and  $r' - i'$  between 0.3 and 1.1 that is clearly seen in the NGC 2403 CMDs, and (2) the bright main sequence stars in NGC 2403 that have  $r' - i' < 0$ . The outer disk of M82 thus lacks the young population that is prevalent in the outer disk of NGC 2403, as expected based on the comparison in Figure 9.



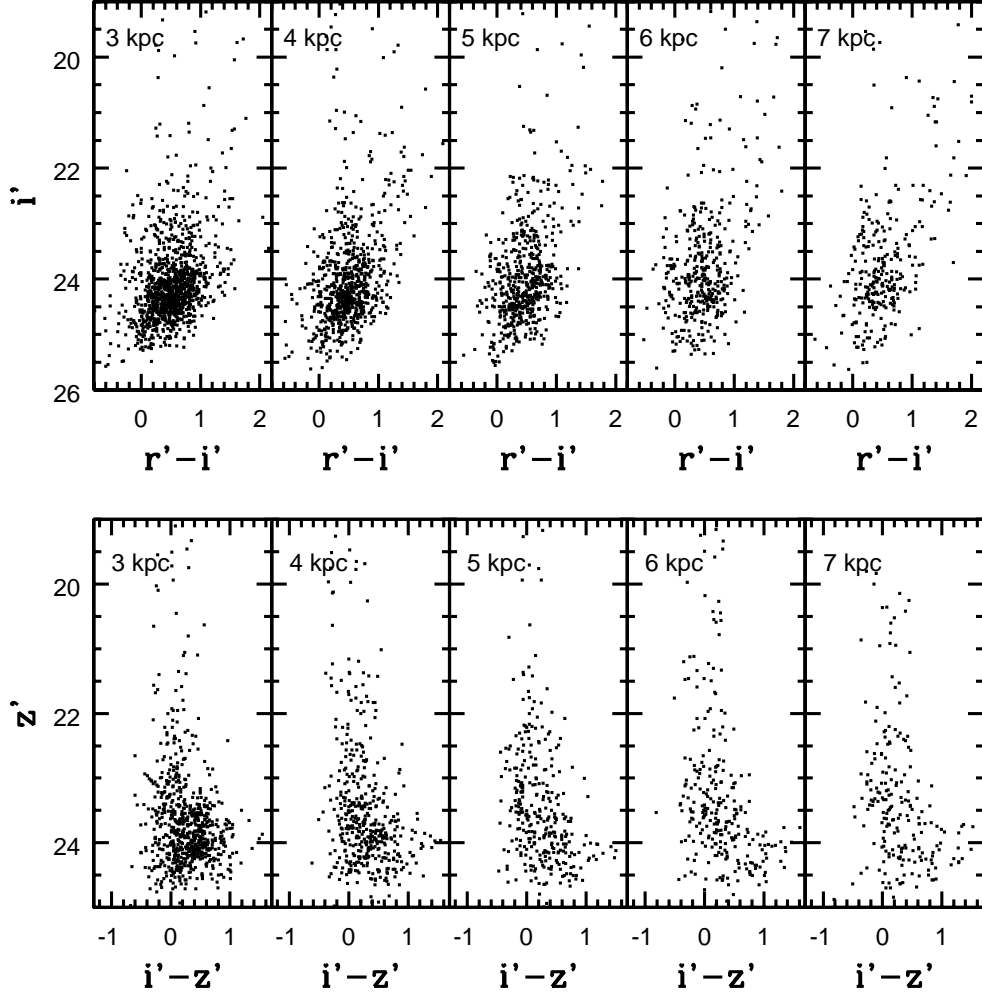


Fig. 11.— The  $(i', r' - i')$  and  $(z', i' - z')$  CMDs of the extraplanar regions of M82. The distance given in each panel is measured from the center of M82 along the minor axis, assuming an ellipticity of 0.68 (Jarrett et al. 2003). Note that a concentration of AGB stars can be traced out to  $D_z = 7$  kpc.

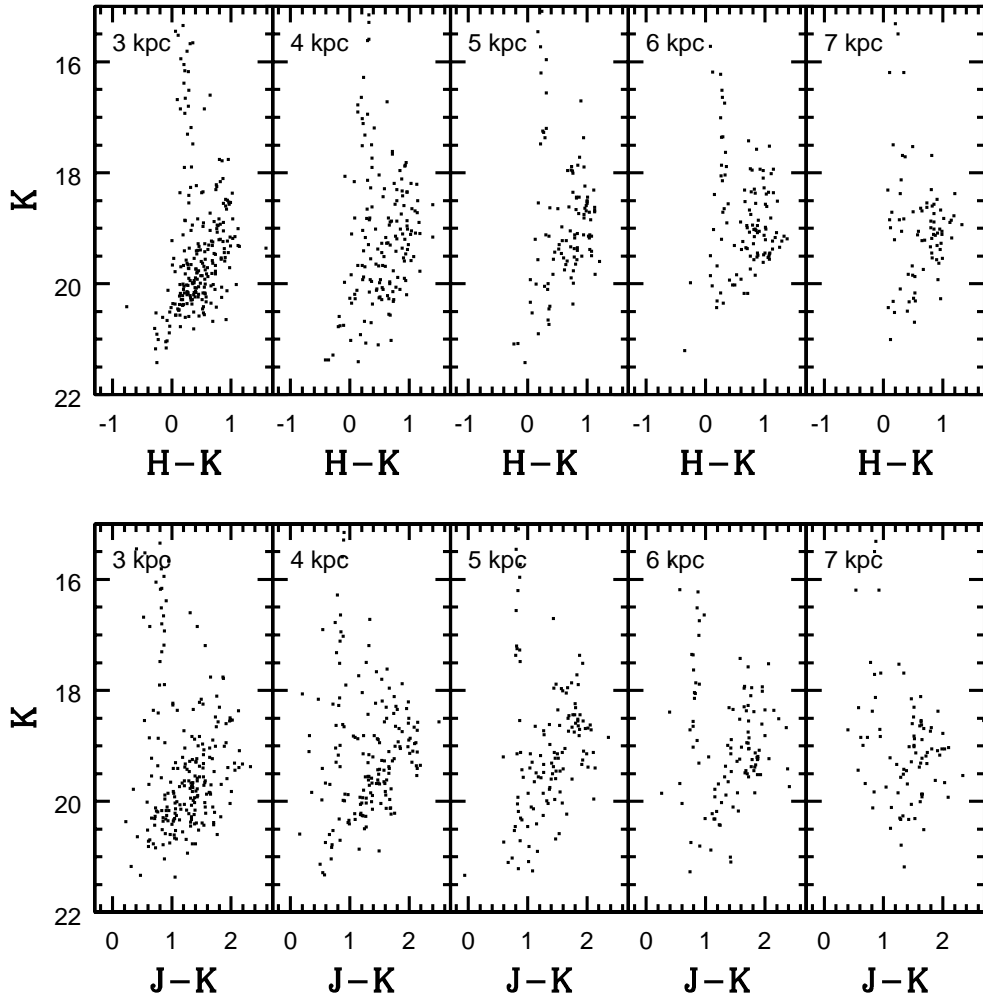


Fig. 12.— The same as Figure 11, but showing the  $(K, H - K)$  and  $(K, J - K)$  CMDs.

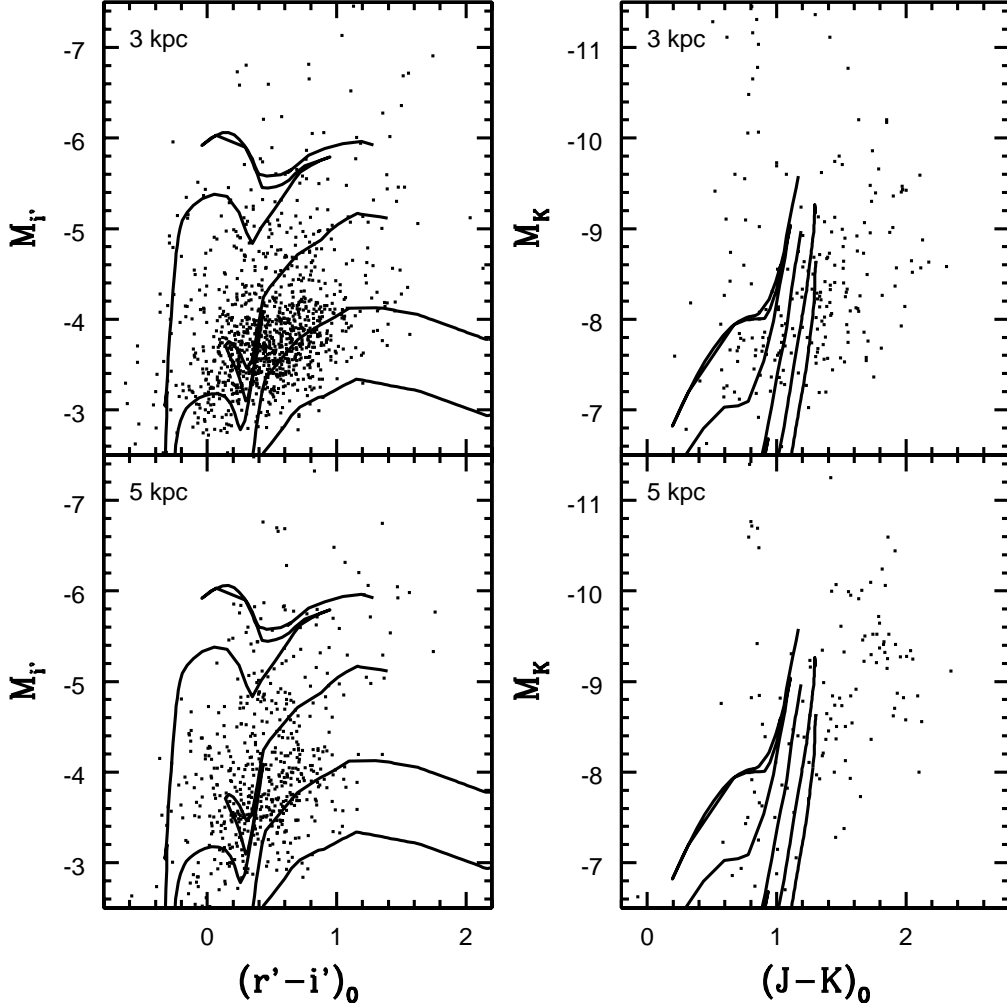


Fig. 13.— The  $(M_{i'}, (r' - i')_0)$  and  $(M_K, (J - K)_0)$  CMDs of the  $D_Z = 3$  and 5 kpc intervals. The solid lines are  $Z = 0.019$  isochrones from Girardi et al. (2002; 2004) with  $\log(t_{yr}) = 7.5, 8.0, 8.5,$  and  $9.0$ . Note that there are (1) blue objects in the  $(M_{i'}, r' - i')$  CMDs that have colors and brightnesses that are consistent with main sequence stars having ages  $< 0.1$  Gyr, and (2) sources that may be RSGs with ages  $< 0.1$  Gyr. The objects with  $(J - K)_0 > 1.6$  in the  $(M_K, J - K)$  CMDs are probably background galaxies.

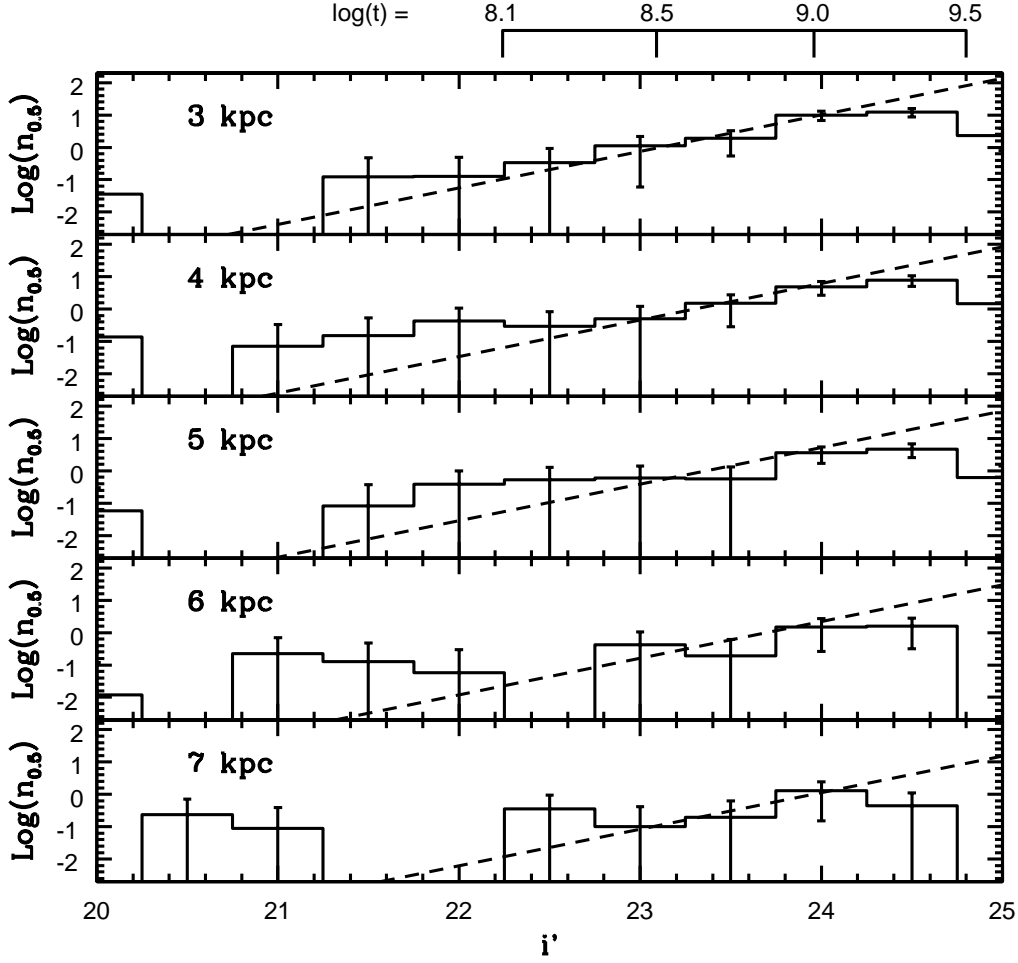


Fig. 14.— The  $i'$  LFs of the extraplanar regions of M82.  $n_{0.5}$  is the number of stars with  $r' - i'$  between 0 and 2 per arcmin<sup>2</sup> per 0.5 magnitude  $i'$  interval. The LFs have been corrected for contamination from foreground stars and background galaxies using number counts in the control fields. The dashed line shows the reference SF relation from Figure 7, shifted to match the number of stars with  $i' = 23, 23.5,$  and  $24$  at each  $D_Z$ . The peak AGB brightnesses in the Girardi et al. (2004)  $Z = 0.008$  models are shown at the top of the figure, and this calibration suggests that significant numbers of AGB stars with ages  $\text{log}(t) \sim 9$  are detected out to  $D_Z = 7$  kpc.

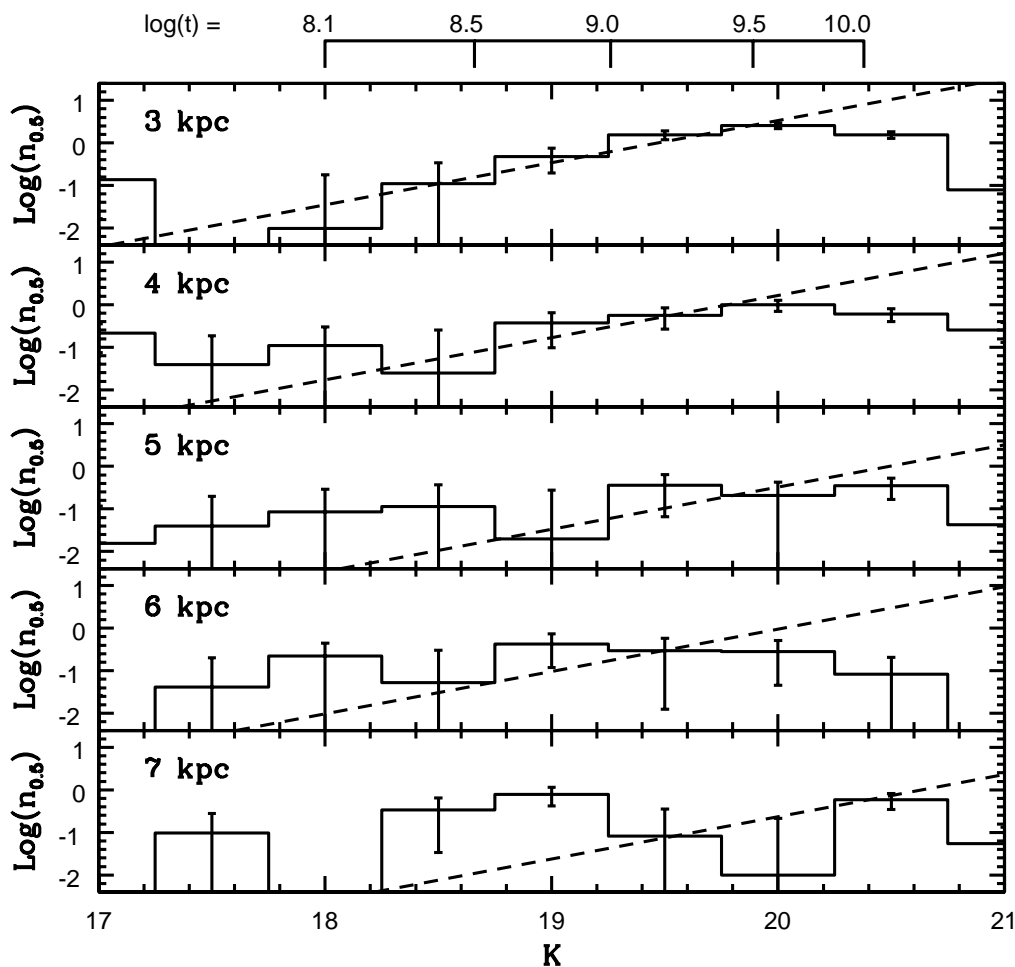


Fig. 15.— The same as Figure 14, but showing the  $K$  LFs of stars with  $H - K$  between 0 and 1 in the extraplanar regions of M82. The dashed line shows the reference SF relation from Figure 8 but shifted to match the number of stars with  $K = 19, 19.5,$  and  $20$  at each  $D_z$ . The peak AGB brightnesses in the Girardi et al. (2002)  $Z = 0.008$  models are shown at the top of the figure.

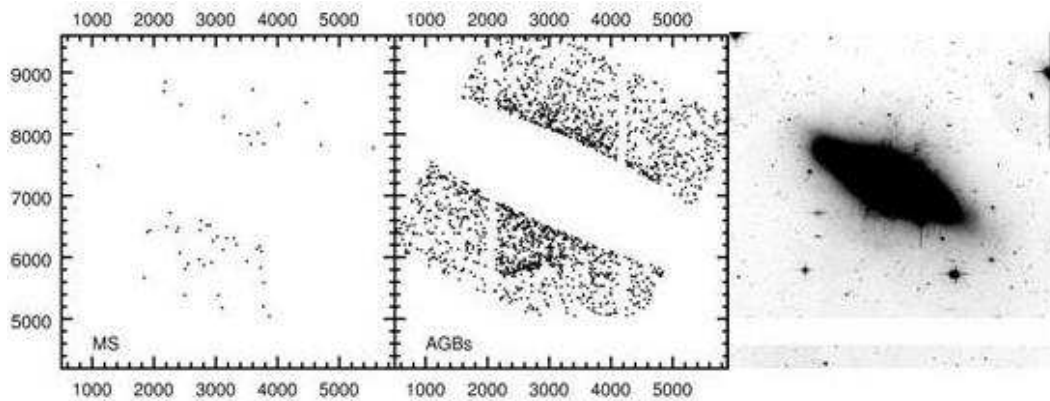


Fig. 16.— The spatial distribution of extraplanar objects with photometric properties that are consistent with either main sequence (MS) stars or AGB+RSG stars. Each panel covers  $16 \times 16$  arcmin<sup>2</sup>, and the corresponding section of the MegaCam  $i'$  image is also shown. The co-ordinates are in pixel units. Note that the MS and AGB stars are concentrated along the minor axis of the galaxy, and that there is a tendency for the number densities of both types of objects to drop with increasing distance from the disk. The density of MS and AGB stars is higher to the south of the disk than to the north. M82 South is the compact collection of AGB stars to the south of the main body of M82, at  $(x,y) = (2600,6000)$ .

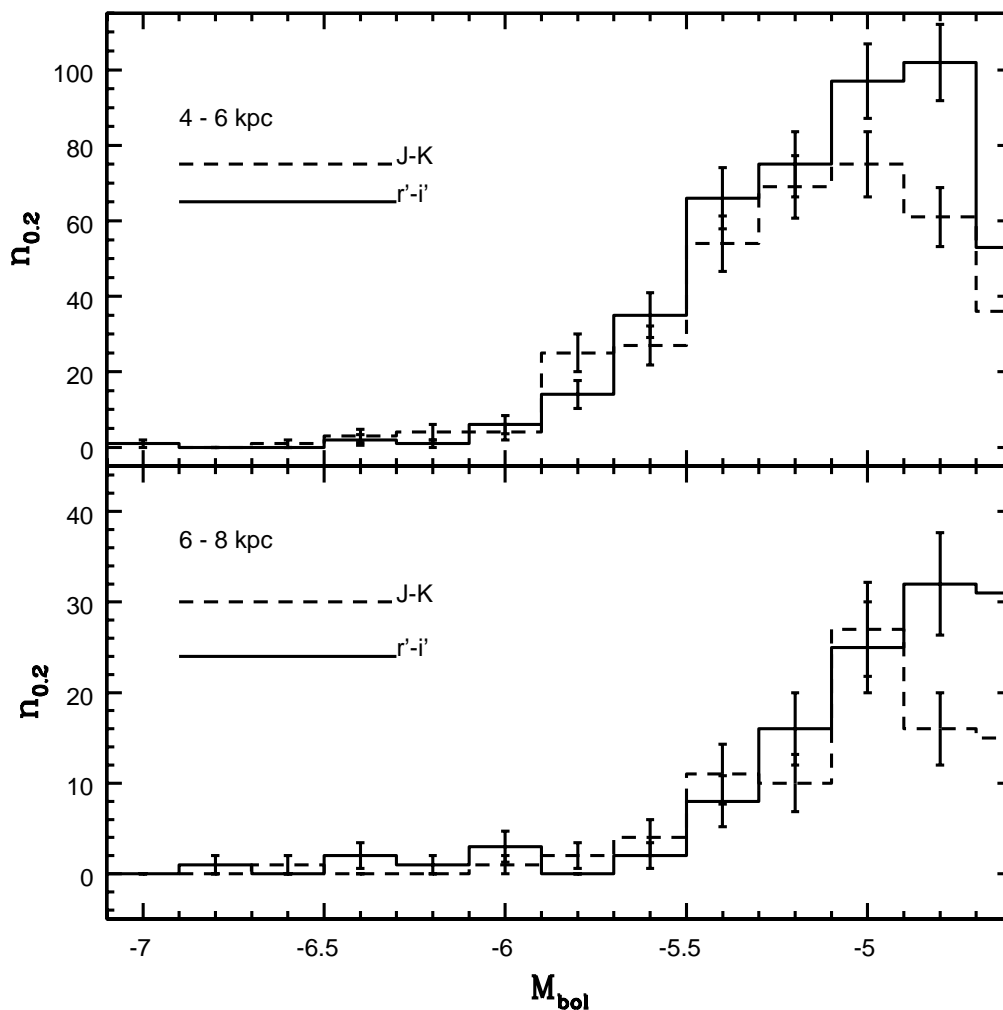


Fig. 17.— The bolometric LFs of objects with  $\log(T_{eff})$  between 3.54 and 3.60 constructed from the  $(i', r' - i')$  (solid line) and  $(K, J - K)$  (dashed line) CMDs.  $n_{0.2}$  is the number of stars per 0.2 mag interval in  $M_{bol}$ . The good agreement between the LFs constructed from the MegaCam and WIRCam data suggests that blending does not affect the bright AGB stellar content in the MegaCam images.